Near-Frictionless Carbon Coatings for Spark-Ignited Direct-Injected Fuel Systems

Final Report, January 2002

Jeff Hershberger, Orhan Öztürk, Oyelayo O. Ajayi, John B. Woodford, Ali Erdemir, George R. Fenske

Tribology Section, Energy Technology Division, Argonne National Laboratory

Support for this project came from Rogelio Sullivan of the Office of Advanced Automotive Technologies (OAAT) within the U.S. Department of Energy's Office of Transportation Technologies (OTT).

EXECUTIVE SUMMARY

This report describes an investigation by the Tribology Section of Argonne National Laboratory (ANL) into the use of near-frictionless carbon (NFC) coatings for spark-ignited, direct-injected (SIDI) engine fuel systems. Direct injection is being pursued in order to improve fuel efficiency and enhance control over, and flexibility of, spark-ignited engines. SIDI technology is being investigated by the Partnership for a New Generation of Vehicles (PNGV) as one route towards meeting both efficiency goals and more stringent emissions standards. Friction and wear of fuel injector and pump parts were identified as issues impeding adoption of SIDI by the OTT workshop on "Research Needs Related to CIDI and SIDI Fuel Systems" and the resulting report, Research Needs Related to Fuel Injection Systems in CIDI and SIDI Engines.[1]

Argonne's approach to these friction and wear issues was to investigate the applicability of NFC to fuel system parts. In collaboration with Delphi Automotive Systems and BP Amoco plc, Argonne carried out two tasks: optimize the deposition of NFC onto standard flats and balls as well as production fuel injectors, and perform both industry-standard lubricity tests and customized wear tests designed to simulate the engine environment. These tests were performed with several gasolines and other fuels, and the NFC performance was compared to that of uncoated parts and other commercially available coatings, all applied to production fuel injectors. Finally, to understand the wear mechanisms, Argonne applied advanced characterization techniques to the worn and unworn coatings, the steel against which they wore, and the wear debris. The industry-standard lubricity tests included the Falex ball-on-three-disc (BOTD) test, while the customized wear testing was performed in a sealed reciprocating system designed to perform fretting wear tests. Long-duration reciprocating tests were performed with a

total sliding distance of 2 km in order to determine the steady-state performance of the NFC coatings. The worn surfaces were examined by 3D optical profilometry to determine wear rates. The advanced characterization methods applied included Raman spectroscopy and laser scanning measurement of residual stresses in the NFC coatings.

In the customized reciprocating tests, comparisons between two varieties of NFC and three commercially available diamondlike carbon (DLC) coatings showed that the NFCs gave consistently high performance and were generally the best choice for reducing friction and wear, although one of the commercial DLCs achieved performance comparable to the NFCs in several individual tests. The other commercial DLCs displayed poor performance under certain conditions. In dry or ethanol-lubricated wear, NFC6 performed the best; when subjected to E85 or M85 fuel, the commercial DLC gave the best results; and NFC2 displayed the lowest friction and wear rate of the three in regular gasoline, the most relevant condition for fuel injector applications. NFC2 reduced friction in all the liquids tested, compared to tests of uncoated materials in the same fluids; NFC6 did also but not to as great an extent.

The long-duration tests designed to determine the ultimate wear lifetime of the NFC coatings on injectors in current- and next-generation gasolines showed that NFC6 provided 27% lower friction, while NFC2 reduced friction by nearly a factor of two, after averaging over the seven formulations of gasoline tested. In addition, NFC provided clear improvements in total wear rate and wear rate of the steel flats compared to the uncoated injectors. In the case of the coated injectors themselves, NFC6 provided reductions of both friction and wear, while the NFC2 coating provided extremely low friction and counterface wear by slowly sacrificing itself. This may ultimately be beneficial in applications where the geometry of the mating (uncoated) part is of paramount importance, for example, the nozzle of a fuel injector carefully shaped to

control the fuel spray characteristics. Analysis of the data from these long-duration tests also showed that the major factor influencing both the friction and the wear was the coating, not the gasoline.

The standardized BOTD lubricity tests were in general agreement with the customized reciprocating tests as to the benefit of using NFC coatings in an engine environment. The lubricities of the formulated gasolines tested with uncoated BOTD discs were also consistent with the wear rates observed in reciprocating wear tests using uncoated materials. In this way, the testing methods employed here have been shown to be self-consistent, and they can be compared to results from other labs.

The wear mechanisms operating in these tests were consistent with the analysis of residual stresses in the NFC coatings. The low-magnitude compressive residual stresses in the NFCs retarded crack opening but were too small to cause spallation or delamination. Raman characterization of unworn surfaces and surfaces worn in gasolines did not produce any evidence of a transfer film originating from the NFC, either on the steel flat or on the exposed steel substrate. The Raman data also did not show any graphitization of the NFC during wear, supporting the hypothesis that the wear mode of the NFC in gasoline was mechanical polishing rather than phase transformation.

This work is relevant to several aspects of the current research needs of the OAAT SIDI program. It has been shown that wear and fatigue issues arising from rate shaping, multiple injections, and other diesel-like strategies can be addressed by NFC or other coatings. This work may be regarded as enabling the pursuit of those design options by showing that NFC coatings are compatible with the other demands on fuel injectors. In addition, this work directly addressed issues in injector materials and parasitic losses by investigating the effect of fuel

additives on friction and wear and attempting to reduce friction in gasoline-lubricated parts, which certainly include those not exposed to combustion, such as pumps. Scale-up to industrial-coating throughput rates is being addressed in order to offer NFC coatings to parts' manufacturers. This work has shown that NFC is a viable and valuable technology for SIDI fuel systems, and the authors hope that NFC will help hasten the adoption of SIDI technology in the U.S. marketplace.

TABLE OF CONTENTS

LIST OF TABLES AND FIGURES

I. INTRODUCTION

A. Spark-Ignited, Direct-Injected Engine Technology

Spark-ignited, direct-injected (or SIDI) engine technology refers to a system of delivering fuel to the combustion chambers of an engine without mixing it with air beforehand. Spark-ignited engines, which typically run on gasoline, are to be contrasted with compression-ignited (or CI) engines, which typically run on diesel fuel. Direct injection (DI) is to be contrasted with port fuel injection (PFI), the most common type of fuel system found in passenger vehicles, in which fuel and air are premixed before introduction to the cylinder.

Gasoline engines are used in applications ranging from handheld landscaping tools to municipal electrical power facilities. Direct injection is in use in electrical generators and was first included in motor vehicles by Mitsubishi Corp. The objective of developing DI fuel systems in SI motors is to achieve increased fuel efficiency while maintaining the low emissions character of SI engines. However, DI motors are highly sensitive to formation of solid deposits on the fuel injectors. Other issues in SIDI development include tailpipe emissions, which are not yet an improvement over PFI systems, and injector design challenges (such as tribological issues) posed by the low lubricity of gasoline and the high fuel injection pressures required for proper dispersal of the fuel in engine cylinders. When researchers overcome these obstacles, SIDI technology promises greatly improved fuel control compared to PFI systems.

B. Near-Frictionless Carbon Coatings

Near-frictionless carbon (NFC) coatings are a surface treatment designed to reduce friction, wear, and catastrophic failure of contacting surfaces in relative motion. The NFC series of coatings was invented at Argonne National Laboratory (ANL) and belongs to a class of

coatings known as amorphous diamondlike carbon (DLC), which are under development primarily but not exclusively for their mechanical properties. The NFC coatings are named for their behavior in wear tests in the presence of inert gases, where they display friction coefficients as low as 0.001, among the lowest recorded for solid-solid contact. NFCs also show greatly reduced rates of material removal in wear tests when compared to uncoated materials.

Adoption of NFC coatings in space and inert environments such as pumps is proceeding. Scale-up of the coating process from research-level throughput to industrial quantities is also in progress with ANL's acquisition of an industrial coating system for conversion to NFC production. The process by which NFC coatings are deposited is vacuum-based. As a result, the substrates to be coated cannot be volatile. No heating is involved, so temperature-sensitive substrates are not damaged by the process, and the coatings are sufficiently thin that mechanical tolerances of coated parts are not affected. NFC coatings, like other DLCs, are temperature sensitive and lose their superior tribological properties above approximately 250ºC. For applications meeting these conditions, the low wear rates of NFCs and of the materials worn against them make them an attractive candidate for solution of tribological problems in the mass market.

C. DOE Passenger Vehicle Engine Research Programs

This project grew out of the Office of Advanced Automotive Technologies (OAAT) participation in the Partnership for a New Generation of Vehicles (PNGV) effort. The PNGV is a long-term partnership whose goals include helping automakers to bring to market a passenger car possessing the functional specifications of a 1994 family sedan but achieving 80 mpg fuel

economy and drastically reduced emissions of unburned hydrocarbons (HC), nitrogen oxides (NO_x), and particulate matter.

The OAAT's research programs in SIDI are focused on three barriers to its commercialization in the United States. First, the EPA's proposed Tier 2 emissions standards, which will come into effect in 2004, include limits on emission of HC, NO_x, and particulate matter. Current SIDI designs meet limits on particulate emission but require further work to meet HC and NO_x limits. The high sulfur content of U.S. gasoline compared to European and Japanese gasolines is one reason. Strategies being pursued to meet SIDI emissions limits include more advanced combustion control and exhaust aftertreatment technologies.

The second barrier to U.S. adoption of SIDI is the high cost of the fuel system hardware required. Direct injection requires the addition of a high-pressure fuel pump to achieve the desired spray characteristics when gasoline is injected into the cylinder and mixes with the air there. In addition, the fuel injectors themselves must meet more stringent design criteria due to their operation at higher pressures and in the more aggressive environment of the combustion chamber. Research towards overcoming this barrier includes this work, which seeks to improve the reliability and lifetime of injectors and pump hardware experiencing wear in gasoline. Ensuring the long lifetime of parts constructed with inexpensive base materials may allow simplification of the fuel system, and the reduced tendency for NFC-coated surfaces to bind may allow relaxation of design tolerances and, therefore, reduce production costs. Other research into cost reduction includes a program on fuel management systems.

Third, the fuel efficiency of SIDI systems is an improvement over that of port fuel-injected gasoline engines but does not yet meet PNGV goals. At the OTT workshop on "Research Needs Related to CIDI and SIDI Fuel Systems" held at Argonne in March of 2001, it

was noted that one impediment to SIDI efficiency is frictional losses in the high-pressure fuel pump. These losses can offset half of the fuel savings gained by the use of DI technology. Research on the performance of NFC-coated components in gasoline environments is also relevant to this barrier, since reduction of friction between key parts in fuel pumps may provide a direct recovery of miles per gallon for the vehicle as a whole.

A report on the findings from that workshop, Research Needs Related to Fuel Injection Systems in CIDI and SIDI Engines, gave future directions for research related to this work. This OTT report stated that the research needs related to SIDI fuel systems were grouped within the following eight areas, listed in order of priority:

1. **Injector Design**
2. **Combustion**
3. **Deposits**
4. **Modeling**
5. **Fuels**
6. **Materials**
7. **Parasitics**
8. **System Integration**

This project is relevant to several of the above listed needs. For injector design (1), one of five research topics was to investigate the feasibility of using rate shaping and other diesel-like injection strategies. This will require attention to wear or fatigue due to additional contacts per cycle. For the combustion area (2), one of the three research topics was to develop fuel additives and/or coatings to prevent deposits from forming on the injector tip.

All five research topics in the materials area (6) were informed by this work. They were as follows. First, determine the effect of sulfur and additives on fuel lubricity. Second, develop a procedure for quality control of coatings. Third, scale up a process for producing DLC coatings to reduce cost. Fourth, determine the role of sulfur, fuel additives, and alternative fuels (E85 and M85) on corrosion of fuel-system components. Finally, investigate various materials

in terms of inherent resistance to formation of deposits. In addition, the decreased friction found with use of NFC films is highly relevant to the parasitics area (7), whose research objective is to develop ways to reduce the parasitic energy losses in the low-pressure intake pump, high-pressure engine-drive pump, and air pump.

II. REVIEW OF THE LITERATURE

This review of relevant literature is split into three parts. The first is on research into SIDI systems, the second is on application of coatings in engine systems, and the third is on research into NFC coatings. The literature on research into SIDI systems is split into three parts: injector design, combustion and motion of fuel and air, and tribology.

A. SIDI Research

1. Injector designs

In the area of injector design, Lee et al. analyzed the shape of the gasoline spray from an injector as a function of various parameters and found that the injection pressure of the fuel is an important factor[2] in that higher pressure sprays are more effective. In this paper, pressures of only 5-7 MPa were considered, whereas in other papers considerably higher pressures were investigated. Henriot et al. discussed a 3-D computational fluid dynamics model being used to design an engine around a DI injector.[3] They noted that inclusion of an injector (previously behind the port of a PFI design) in the cylinder head of an SI engine is not a trivial task. The injector and spark plug must be placed such that the spray develops and can be ignited by the spark, while leaving room for the ports. Li et al. studied HC emissions from SIDI engines and found that a strong contribution came from liquid fuel which reached the cylinder walls and piston.[4] They also concluded that, while wetting on the exhaust side of the liner was worst from

an emissions standpoint, all liner locations were probably highly undesirable because of oil-layer dilution and subsequent wear of the liner and rings. Previously, Habchi et al. had found that a liquid film or pool of gasoline tended to form on the piston of an SIDI engine.[5] Up to 25% of the injection charge remained liquid during cold operation or cold start, affecting efficiency as well as emissions.

There have also been reviews of SIDI systems, in general, and emissions, in particular. An excellent review of the history of research and literature on SIDI was performed by Zhao et al..[6] Hill and Smoot reviewed the chemical pathways for formation and destruction of NO_x compounds emitted by engines.[7] Similarly, Richter and Howard summarized the work on the formation of particulate emissions starting from polycyclic aromatic hydrocarbons.[8] The measurement of particulate emissions was explored in a paper by Hall and Dickens.[9] This paper highlighted the differences between techniques used by different labs to measure engine soot output.

2. Combustion and motion of fuel and air

The second part of the literature on SIDI systems is the combustion and the motion of fuel and air, or mixture preparation. The flow of fuel inside a high-pressure swirl-type DI injector was investigated by Cousin et al. using simulations.[10] They found that the spray-cone sheet thickness near the orifice strongly affects the mixture preparation. This finding argues for careful control of the orifice geometry against effects such as deposit formation and wear. A presentation on optical flow characterization by Hentschel described in detail the droplet size and other aspects of in-cylinder mixing.[11] The injectors he discussed were also of the high-pressure swirl type and used pressures up to 12 MPa. Optical diagnostics were also used by Wicker et al.

in a paper on fuel spray structure.[12] They noted that SIDI engines require more precise control of both fuel and spark than do conventional PFI engines. They discussed the inhomogeneities of jets and sprays caused by the details of liquid flow within the injector. They also noted that preferential concentration and directed motions of fuel in SIDI engines are significant, suggesting a need for attention to the geometry of the internal surfaces of the injector and its orifice.

3. Tribology

The third part of the literature on SIDI work is the area of tribology, or friction and wear. Several papers have been published on fuel lubricity, especially since the experience of Sweden and Canada after reformulation of diesel fuel caused fuel pump failures. Wei et al. discussed the lubricity of gasolines and found that the poor wear-protection properties of gasoline relative to diesel was primarily due to gasoline's low viscosity.[13] Some of the same authors had previously compared the lubricating properties of gasoline and diesel.[14] They explored the effects of detergents and other additives. Diesel lubricity additives were found to have a similar function in gasoline. In 1999, Nikanjam reviewed the work to date on providing a specification for the lubricity of diesel fuel.[15] The discussion centered around the effects which removal of environmentally harmful components such as sulfur would have on the lubricity of diesel. This information is highly relevant to discussions of SIDI engines since diesel fuels also operate in direct injection. A standard for assessment of diesel lubricity was given by ISO12156-1 and -2, which specified a set of wear test conditions in a high frequency reciprocating rig (HFRR) and a maximum wear scar size for acceptable lubricity.[16] Further remarks on wear in injectors due to the lubricity of fuels are found in a study by Lacey.[17] That work found that oxidative corrosion

was the predominant mechanism of wear in very highly processed fuels, leading to catastrophically high wear rates. In 1999, Bardasz et al. compared the lubrication and wear performance in a test study of several SIDI and PFI engines.[18] They observed significant piston bore wear under some conditions, and suggested that soot was the cause.

Many investigations of friction, wear, and lubrication have been performed for non-DI gasoline-engine applications. Tung and Tseregounis developed a method for simulating piston liner-ring wear in a HFRR wear tester.[19] Using direct measurement techniques, Wakuri et al. studied the total frictional loss in an engine, as well as the friction in the piston assembly and between the cam and follower.[20] A study on valve seats and inserts for heavy duty diesel engines by Wang et al. was notable for its encyclopedic coverage of failures.[21] They performed microscopy on over 100 valves from 47 engines. Wear and failure due to adhesion, corrosion, abrasion, and delamination from mechanical or thermal fatigue were observed. Ito et al. studied cam wear using an engine-mountable friction measurement device.[22] Many novel experimental techniques such as these have been adopted to reduce the dependence of engine manufacturers on full-scale engine tests, which are time-consuming and expensive.

B. Application of Coatings to Engine Parts

The section of this literature review devoted to the application of coatings to engine parts is divided into two parts: thermal barrier and wear-resistant coatings.

1. Thermal barrier coatings

A study by Gorel et al. reported an engine test of a thermal barrier coating applied to surfaces inside the combustion chamber, including the piston crowns.[23] The coatings were intended to reduce particulate emissions, although no fuel economy improvements could be

associated with coatings applied in the cylinder. Thermal barrier coatings were also attempted for control of unburned hydrocarbon emissions from a homogeneous charge-compression ignition engine, as reported in a paper by Hultqvist et al.[24] However, the emissions actually increased due to flame quenching; the coatings being catalytic may have contributed to this problem.

2. Wear-resistant coatings

On the subject of wear-resistant coatings, an overview of one manufacturer's DLC coatings for automotive applications is given by Gahlin et al.[25] A paper by Erdemir et al. describes the wear resistance of Argonne's NFC coating in diesel fuels with a variety of sulfur levels, including the low-lubricity, low-sulfur fuels which are desired for environmental protection.[26]

C. NFC Research

The third part of this literature review discusses NFC coatings. It is split into three parts, the first of which covers the NFC deposition process and how it has been refined. Also covered is basic research and bench wear-testing.

1. Deposition process

In 1994 Erdemir et al. experimented with ion-beam-deposited DLCs and concluded that the friction coefficient of 0.05-0.07 in laboratory air is due to the formation of a carbon-rich transfer film.[27] Meletis et al. deposited those films on nitrided steels and found that the reduced substrate deformation improved the lifetime of the film.[28] Later, Liu et al. investigated the load

and speed dependencies of the graphitization-transfer process.[29] They cited hydrogen depletion of the sp3 atomic structure of the DLC and described the transformation kinetics analytically.

In 1997 a crucial step was taken by Erdemir et al. by forming DLC films from source gases including methane, acetylene, and combinations of hydrogen and methane.[30] Friction coefficients as low as 0.01 were measured in dry nitrogen environments. Further studies explored the effect of source gases on tribological properties.[31, 32,33] Later, high-temperature chlorination of silicon carbide was explored as a route towards DLC film creation, resulting in a disordered graphitic surface layer.[34]

2. Basic research and characterization

The second part of the literature on NFC coatings covers basic research into the coatings' structures and properties. Raman spectroscopy and electron microscopy were used by Erdemir et al. to study the transfer films formed by ion-beam-deposited DLCs.[35] Later studies included transmission electron microscopy and infrared spectroscopy, and concluded that some graphite was being formed during wear of those DLCs.[36,37] The effect of applying the ion-beam DLCs to hard zirconia substrates was also investigated by Erdemir et al.[38] The influences of humidity and temperature were reported later by Liu et al.[39]

Modern NFC films, made from hydrogen-enriched plasmas, were investigated by Erdemir et al., who found friction coefficients as low as 0.003.[40] Heimberg et al. reported on the time and speed effects involved in this superlow friction coefficient.[41] They found that friction changes in NFCs could be explained by gas adsorption kinetics. Raman spectroscopy, transmission electron microscopy, and other techniques were used to describe the structure of the coatings, transfer films, and wear debris of the NFCs.[32,33,39]

3. Bench wear testing of prototype parts

The third part of the NFC literature covers the results of bench wear testing of prototype parts and the mechanical capabilities of the coating. Aside from the many discussions of friction and wear rate reduction in the references cited above, Erdemir and Fenske studied the high-temperature performance of both diamond and DLC films.[42] The diesel-lubricated scuffing performance of NFC coatings was investigated by Ajayi et al., who found that coated surfaces would scuff only at contact stresses high enough to deform the substrate and delaminate the film, or after the NFC was removed by wear.[43] The scuffing performance of NFC in dry sliding conditions was then tested by Alzoubi et al.[44] Again, NFC was found to provide an improvement in scuffing resistance of two orders of magnitude.

III. APPROACH

A. Deposition and Optimization of NFC Coatings on Fuel Injectors and Steel Parts

To test the effectiveness of NFC coatings to reduce wear and improve lifetime of SIDI fuel system parts, we coated steel balls and flats as well as production fuel injectors with NFC for wear testing. The results of the NFC coating process, plasma-assisted chemical vapor deposition (PACVD), depend on variables such as the method used to mount the substrates in the coating chamber, the amount of power fed to the system, etc. These variables affect the deposition rate and the uniformity of the coating from area to area on an oddly shaped part. The PACVD technique is not line-of-sight, so three-dimensional parts can be coated, but certain geometries pose special challenges. For example, the interior diameter of a tube can create a resonance in the plasma. For this study, standard steel balls and flats were coated in the same

manner as previous research samples. Fuel injectors used in this work required special attention for mounting and adjustment of deposition rates.

B. Industry Standard Wear Testing

Standardized bench tests for friction, wear, and lubricity are used in industry for rapid turnaround when large numbers of materials, fuels, or lubricants must be evaluated. Such tests do not provide detailed information or a perfect correspondence to service conditions, but they give a figure of merit for comparisons, particularly between laboratories. In Europe, standards ISO12156-1 and 12156-2 cover testing methods and limits for lubricity of diesel fuels, while in the United States, the Falex BOTD test is under consideration as a standard test for fuel lubricity. The ISO12156 test uses a reciprocating steel-ball-on-steel-flat wear configuration, while the BOTD tester uses an alumina ball rotating unidirectionally against three steel flats set at right angles. This study has used the BOTD test to evaluate all coatings and fuels, and the custom wear-testing described below is similar to the specifications of the ISO12156 test. To check the chemical compatibility of the NFC coatings with a variety of fuels, a large number of gasolines and alternative fuels were used in these tests.

C. Customized Wear Testing

To more closely approximate the tribological conditions encountered by the part in service without resorting to expensive engine tests on each combination of coating and fuel, specialized custom wear tests were devised for this work. A reciprocating wear tester built for studies of high-vapor-pressure CIDI fuels was modified to accommodate prototype SIDI fuel injectors and fuels. The contact pressure, speed, and duration of the tests were chosen to

simulate engine conditions, including lifetime durability tests of one million cycles. The same large variety of fuels tested in the BOTD tests were evaluated in reciprocating wear.

D. Advanced Coating Characterization

In the process of evaluating the suitability of NFC coatings for this application, the advanced characterization techniques of residual stress analysis and Raman spectroscopy were applied. Residual stress remaining after deposition is a common aspect of coatings, and excessive residual stress, either tensile or compressive, can cause mechanical problems such as cracking or spalling. Residual stress in NFC coatings was determined by a laser scanning system that measured the curvature of a thin, flexible substrate before and after deposition of NFC. Knowing the change of curvature and the thicknesses of the coating and substrate, one can calculate the average stress in the coating using linear elasticity.

Raman spectroscopy was used to elucidate the wear mechanism of the NFCs rubbing against steel in gasolines. Diamondlike carbon coatings exhibit a Raman response with different characteristics depending on the local ordering in the atomic structure of the near-surface material. Changes in the structure of the material, for example wear-induced graphitization, produce changes in the Raman response. Raman spectroscopy was used to determine whether the physical wear mechanism of NFC against steel in gasoline was compatible with the use of NFC in a fuel system.

E. Industrial Collaboration

Argonne worked with two industrial collaborators in this project. Production fuel injectors for this study were supplied by Delphi Automotive Systems. Several varieties of regular and reformulated gasoline were supplied by BP Amoco plc.

IV. EXPERIMENTAL METHODS

A. Coating Deposition

Deposition of NFC coatings was performed in a Perkin Elmer 2400 sputtering system using plasma assisted chemical vapor deposition (PACVD). The system's radio frequency etching mode was used to deliver RF power to the water-cooled substrate table, creating the plasma. This arrangement delivered ion current to the exposed sample surfaces across a DC voltage drop between the plasma (the source of the ions) and the sample surface. The power of the RF supply can be as high as 2000 W for the table and all substrates, and was manipulated to provide the bias between the plasma and samples.

Before introduction to the sample chamber, the samples were ultrasonically degreased and solvent cleaned. Once they were arranged in the chamber, the system was sealed and pumped down to a base pressure of 10^{-6} Torr (1.3×10^{-4} Pa) using a turbopump. Argon gas was introduced into the chamber to achieve a pressure of 10 mTorr, (1.3 Pa), and the RF power to the substrates was ramped up to provide the DC bias for a period of 30 min to sputter clean the sample surfaces. The argon flow and RF power were then stopped, and silane (SiH_4) was introduced into the chamber to achieve a pressure of 3 mTorr (0.4 Pa). The RF power was ramped up to provide the DC bias for a period of 5 min. This procedure creates a silicon-hydrogen plasma and coats the substrates with a layer of amorphous hydrogenated silicon

approximately 100-200 nm thick, which improves adhesion between the substrate and the NFC coating. The silane flow and RF power were then stopped, and methane and hydrogen gas were introduced into the chamber to provide a pressure of 15 mTorr (2 Pa). The ratio of methane flow to hydrogen flow depended on the type of film being deposited; for NFC2, 50% hydrogen was used, while for NFC6, 75% hydrogen was used. The RF power was then ramped up to provide the DC bias for a period of 200-300 min, depending on the coating being deposited. The samples were allowed to cool before venting the chamber and removing them. The resulting coatings were 2-3 μm thick.

B. Ball-on-Three-Disc Wear Tests

A Falex BOTD tester was used to evaluate the lubricity of the gasolines studied. The tester was modified to output its friction force signal to a computer for recording and analysis, which improved calibration of the system. A schematic of the BOTD tester's sample enclosure is shown in Figure 1 on page 23. The drive shaft entering the top of the enclosure held the ball and rotated it against the three discs below it. Friction was measured via a clamp and arm extending to the left, which supported the friction torsion by a load cell. The tester itself is shown in Figure 2 on page 24, where the aluminum sample enclosure is visible in the recessed part of the machine. Tests were performed in a fume hood for safety and odor reduction.

The test conditions were as follows: load, 24.5 N (10 N between the ball and each flat due to geometry); speed, 60 rpm; temperature, 25-30ºC; duration, 45 min; air atmosphere. The discs were 52100 steel with a ground finish (surface roughness R_a = 0.1-0.2 μm) hardened to 57-63 Rockwell C (R_c), and the ball was Al_2O_3 with a diameter of 0.5 in. (1.3 cm) and a surface roughness R_a of 0.008-0.01 μm. Discs to be coated were first polished with alumina slurry with

a grit size of 1 μm. A series of separate tests verified that polishing did not significantly affect the wear scar diameters of uncoated discs. Before testing, the ball, discs, and the parts of the tester which contact the gasoline were ultrasonically degreased and solvent rinsed. After testing, the discs were inspected in an optical microscope, and the diameter of the wear scar (WSD) was recorded for all three discs from each test.

C. Reciprocating Wear Tests

Bench tests to measure reciprocating wear were performed on a customized wear tester called the "Fretting Tester". It was designed for sealed operation with wear track lengths from 0.5 in. (1.3 cm) down to as low as a few micrometers. Having an enclosed volume of approximately 0.5 ft^3 (0.01 m^3), it was ideal for use with volatile liquids such as gasoline. It allowed addition of liquid to the sample cup without opening it to the environment, and could be filled and vented with specific flow rates of any desired gas. In this study, the samples were ultrasonically degreased and solvent rinsed, dried, and placed in the chamber, then the chamber was sealed. The air in the chamber was exchanged with dry nitrogen for 30 min at a flow rate of 10 standard liters per minute. At that point the flow rate was reduced to under 2 standard liters per minute, gasoline was added to the sample cup, and the test was started.

Reciprocating motion was applied to the counterface (ball or fuel injector), which was mounted on a horizontal slider and connected to bellows on the sides of the chamber. The slider was driven through the bellows by an electromagnetic shaker similar to a loudspeaker voice coil. The shaker was driven by a high-current amplifier, which took its drive signal from a frequency generator, generally using a sine waveform. Inside the chamber, the sample resided in a cup for liquids, which was mounted on a lateral load-sensing assembly. The lateral load due to friction

was sensed by a piezoelectric load cell whose sensitivity was approximately 0.001 lb (0.45 g). The cup and load sensor were mounted on a pair of vertical sliders to allow sample exchange. A linear variable differential transformer (LVDT) was used to measure the relative displacement of the sample and counterface; the body was mounted to the sample cup, while the core was attached to the slider and therefore oscillated with the counterface. The normal load was sensed by a load cell on the mechanism used to raise the cup to the counterface. For each test, the load required to raise the cup was zeroed out, and afterwards the sample and counterface were brought into contact, and the normal load between them was measured.

The signals from the LVDT and friction force sensor were displayed on an oscilloscope, which was connected to a computer running a program written in National Instruments's LabVIEW environment. The computer calculated the test duration based on the operator's input, and after the test started, the computer collected 200 digitized dual traces from the oscilloscope throughout the test. Each dual trace contains information from approximately three cycles of oscillation due to the choice of time scale on the oscilloscope. At the conclusion of the experiment, LabVIEW saved the data file containing the traces, and also an abbreviated data file consisting of only the friction values at each cycle number for which data were collected.

The chamber was opened, and the samples removed and cleaned with proper disposal of the gasoline. Both the flat and counterface were then inspected in a MicroXAM 3-D optical surface profiler from ADE Phase Shift. This system reconstructed a three-dimensional (3-D) topographic map of the sample surface, with magnifications and resolutions similar to those of an optical microscope. The system calculated the volume of the areas of the topographical map which lie below the plane of the sample surface, and provided a numerical wear volume in cubic micrometers. The sensitivity of the system enabled wear volumes as small as 1000 μm^3 to be

measured quantitatively. In the case of injectors and balls, whose unworn surfaces are spherical, the system mathematically subtracted the curvature of the sphere from the data set of 3-D heights. It then changed the 3-D rendering from a ball with a flat spot worn into it to a rendering of a flat plane with a hole worn into it. The volume removed from the sphere was then provided in cubic micrometers. Using this system, highly accurate quantitative wear rates for both the flat sample and the counterface were calculated at the same time that the morphology of the worn areas was inspected.

The flats of 440C steel with hardness 60 R_c were polished to R_a = 0.010 - 0.015 μm. Coatings applied to the flats were 1-2 μm thick. The ball counterfaces were 440C steel, 3/8 in. (0.9 cm) in diameter, while the production fuel injectors had a spherical steel tip of 2.85-mm diameter.

D. Raman Spectroscopy

Samples were analyzed using visible Raman spectroscopy, a structural characterization method highly sensitive to the presence of sp^2-hybridized carbon and to the degree of amorphization of the carbon films. This method allowed determination of any potential change in film structure during the wear process. Worn and unworn NFC samples were analyzed. The instrument used had a spatial resolution on the order of a few microns, so it was also possible to characterize particles of wear debris embedded in exposed steel in the wear scars on some of the samples. The NFC film, initially amorphous in structure, is believed to undergo partial crystallization to graphite during the wear process, and Raman spectroscopy allowed us to estimate the degree to which this crystallization took place.

E. Laser Scanning Stress Measurement

The system used to measure the residual stress in NFCs was based on a design by Flinn et al.[45] It consisted of a Class III He-Ne (633 nm) laser, a rotating mirror from Cambridge Technology Inc., a 6-in. (15-cm) diameter lens with a focal length of one meter, and a linear position sensing detector (PSD) from On-Trak Photonics Inc., all mounted on an optical rail and isolated from vibration. The laser beam was reflected from the mirror, which was rotated through a range of angles sufficient to scan the beam across the lens, which was positioned one meter away. Since the focal length of the lens was one meter, the laser beams were parallel behind the lens as they were scanned across it. The sample was placed behind the lens, and its angle was adjusted to reflect the beams back through the lens. The beams were refocused, at a distance approximately one meter from the lens, onto a detector positioned to the side of the mirror. A computer running a program written under LabVIEW manipulated the mirror and read the resulting position of the beam on the detector.

In cases where the sample was completely flat, the refocused laser beam would remain stationary on the detector as the mirror scanned the beam across the sample. A standard sample consisting of a mirrored optical flat was used to verify that the distances between the mirror and lens, and between the lens and detector, were equal to the one meter focal length of the lens. In cases where the sample was not completely flat, for example, if the sample possessed a uniform curvature, the scanned laser beam was refocused at some point in front of or behind the detector, depending on the sign and magnitude of the sample curvature. Therefore, when the laser was scanned across a uniformly curved sample, the beam translated linearly across the detector. The rate at which the beam moved across the detector per distance traveled on the sample gave a quantitative measure of the sample curvature. The sensitivity of the detector was calibrated by

holding two slits a known distance apart against the surface of the detector, and scanning the laser beam across the detector to pass the beam through each. The response was then used to calibrate the signal sensed by the computer. This calibration was verified using a mirrored sample with a large curvature, a concave lens with a radius of curvature of 0.311 m. The system was capable of measuring the curvature of samples with concave or convex radii of curvatures between 3 m and approximately 1000 m.

For these measurements, NFC coatings were deposited onto substrates of Si(100) single crystal wafers cut into 2-in. (5-cm) squares. The curvatures of the wafers were measured both before and after deposition, across two areas of each sample, and in two perpendicular directions. The resulting changes in curvature were used to calculate the average stress in the modified Stoney equation from linear elasticity[46]:

$$\sigma = \frac{E_s t_s^2 \Delta\kappa}{6(1-\nu_s)t_f} ,$$

where E_s and ν_s are the elastic modulus and Poisson ratio of silicon, t_f is the film thickness measured via a cross-sectional image from a scanning electron microscope, t_s is the substrate thickness, and $\Delta\kappa$ is the curvature change. The resulting stress values (in Gpa) were averaged over all four measurements for each sample. Values from different directions were compared to verify isotropy of the stress field. The reported error bars were calculated based on the standard deviation between the stress values, the uncertainty in the film and substrate thickness, and the uncertainty in the curvature change.

V. RESULTS

A. Ball-on-Three-Disc Wear Test with Standard Fuels

A pilot study on the effectiveness of NFC coatings for reducing wear was performed to determine what benefits, if any, might be expected from use of these coatings. Regular gasoline was used in the tests, as well as indolene, E85, and M85 alternative fuels. The results are shown in Table 1 on page 24, giving wear scar diameters (WSD) and wear rates for uncoated discs and discs coated with NFC2. The error values (std) represent the standard deviation of the WSD values from the three discs. Wear rates are given as volume removed per unit load and sliding distance. The formula for volume as a function of wear scar diameter is

$$V = \frac{\pi h}{6}\left(3r^2 + h^2\right),$$

where

$$h = R - \sqrt{R^2 - r^2}\ ,$$

where R is the radius of the sphere and r is the radius of the wear scar.

Figure 3 on page 25 plots the wear scar diameters from Table 1. For all four fuels tested, NFC2 provided an improvement, with regular gasoline showing the largest decrease in wear scar diameter. The corresponding average wear rates are given in Figure 4 on page 26, indicating that the largest wear rate observed for any fuel on a coated sample was smaller than the smallest wear rate observed on an uncoated sample. For regular gasoline, application of a coating to the discs reduced the wear rate by approximately a factor of 70 under these test conditions.

Optical micrographs used to determine the wear scar diameters in these tests are shown in Figure 5 on page 27. They illustrate the wear modes under these test conditions. The worst-case scenario, an uncoated steel disc worn in regular gasoline (Figure 5a), shows signs of abrasive wear from debris. In contrast, changing to M85 fuel (figure 5b) resulted in a polishing wear mode and smaller wear scar. Figures 5c and 5d show NFC2-coated discs worn in the same two

fuels and demonstrate small wear scar diameters. Both images show evidence of delamination of the NFC, where it was thinned by wear close to the circle of exposed metal in the center. This may have been due to the fact that the coating is significantly harder than the steel; in any case, while the coating succeeded in reducing the wear rate of the system, these tests showed that adhesion of the coating to 52100 steel could be improved.

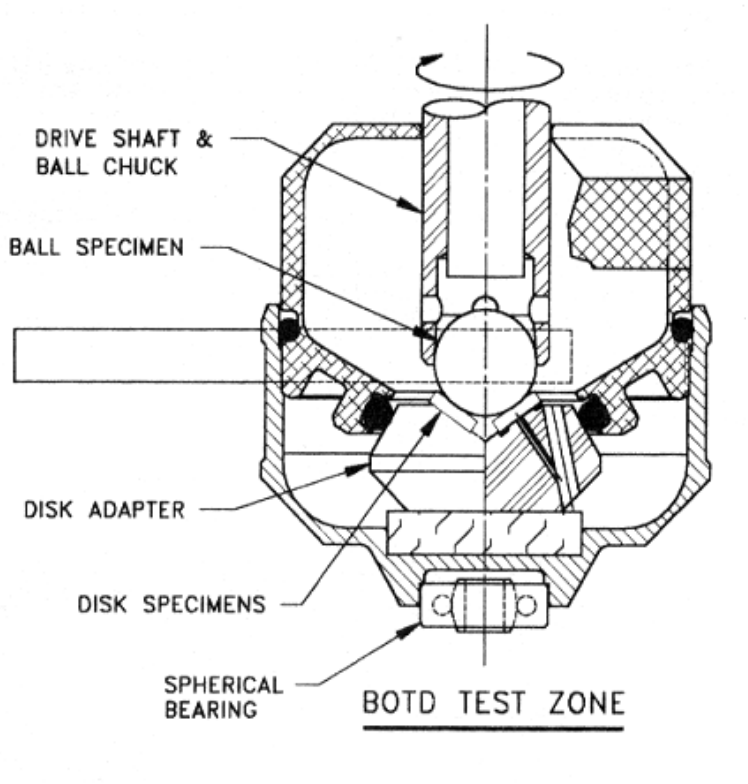

Figure 1. Schematic of the sample enclosure of the Falex BOTD tester.

Figure 2. Photograph of the Falex BOTD tester in a fume hood.

Table 1. Wear scar diameters and wear rates from BOTD testing of uncoated and NFC2-coated discs in several standard gasolines and alternative fuels.

Gasoline Type	WSD ± std (mm) [uncoated]	WSD ± std (mm) [coated]	Wear Rate (mm^3/N-m) [uncoated]	Wear Rate (mm^3/N-m) [coated]
Indolene	0.693 ± 0.032	0.316 ± 0.006	$1.22x10^{-6}$	$5.18x10^{-8}$
Regular gasoline	0.871 ± 0.036	0.301 ± 0.012	$3.03x10^{-6}$	$4.34x10^{-8}$
E85	0.469 ± 0.013	0.318 ± 0.004	$2.54x10^{-7}$	$5.35x10^{-8}$
M85	0.419 ± 0.023	0.356 ± 0.012	$1.64x10^{-7}$	$8.46x10^{-8}$

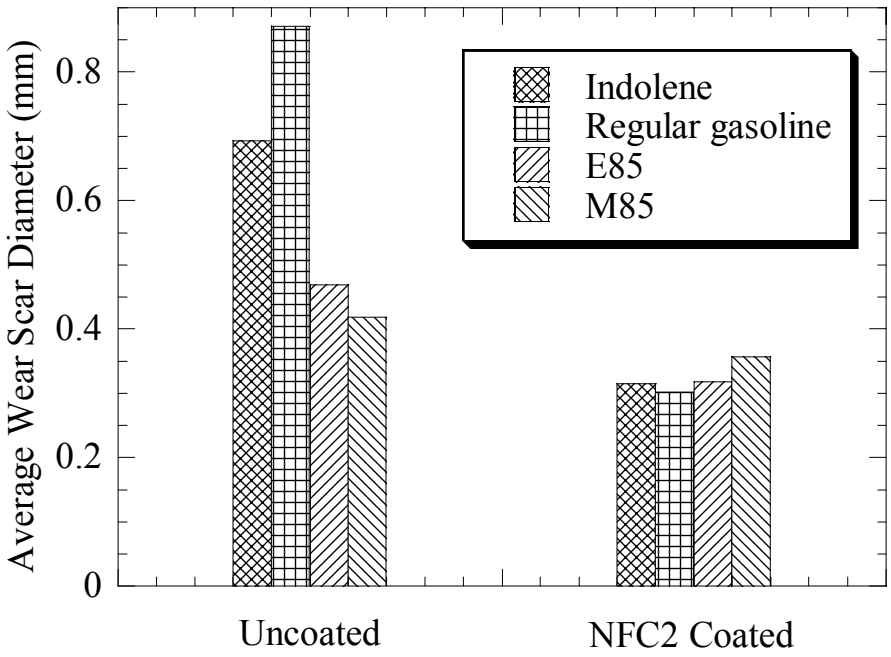

Figure 3. Wear scar diameters of uncoated and NFC2-coated discs from BOTD tests in four fuels.

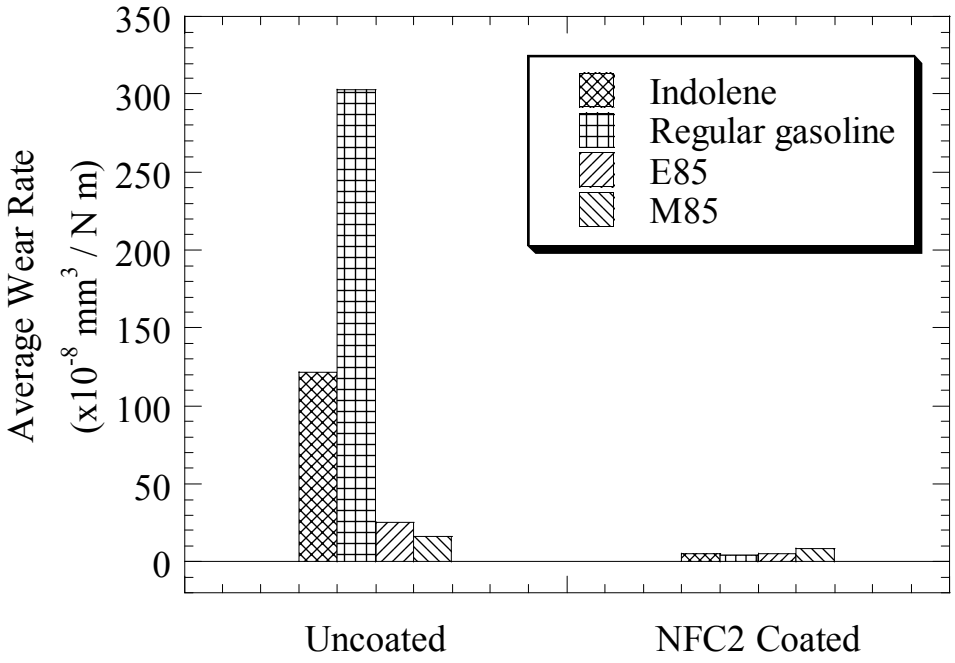

Figure 4. Average wear rates for uncoated and NFC2-coated BOTD discs tested in four fuels.

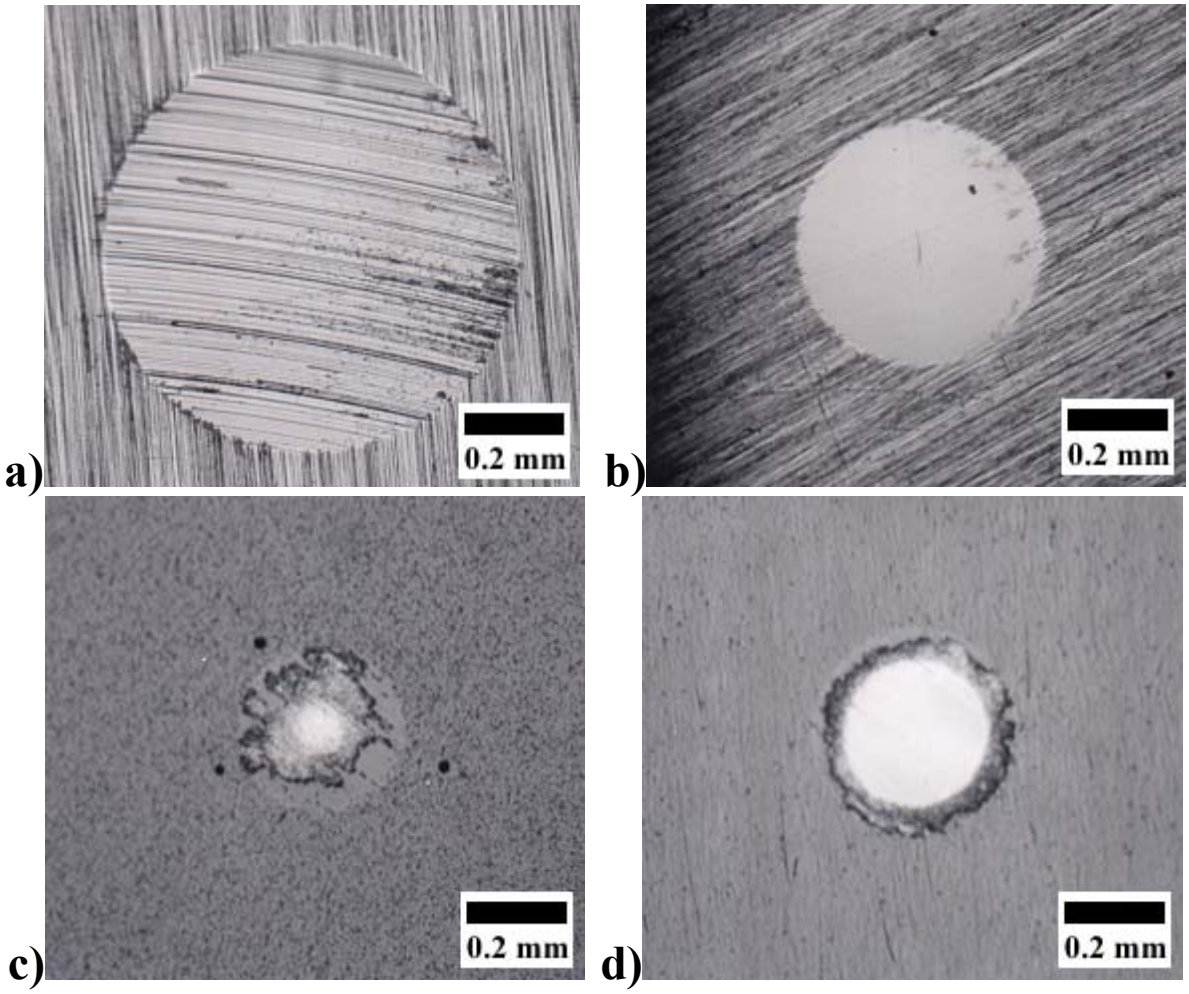

Figure 5. Optical micrographs of uncoated BOTD discs worn in (a) regular gasoline and (b) M85 fuel. Images (c) and (d) are of NFC2-coated discs worn in the same fuels, respectively.

B. Initial Reciprocating Tests

Reciprocating tests were performed to allow a more accurate simulation than BOTD for engine parts such as fuel injectors. Fuel injectors experience reciprocating, not unidirectional, wear, and the oxygen-poor combustion chamber is better simulated by a dry nitrogen environment than by laboratory air. In this exploratory study, regular gasoline was the fuel used, with ethanol included in the tests as a control. The wear behavior of the surfaces in an unlubricated condition, with laboratory air, was also tested as a worst-case scenario. This gauged the effectiveness of the coatings in protecting against failure in unlubricated engine operation.

The testing was performed with a stroke length of 200 μm and a duration of 100,000 cycles, giving a total sliding distance of 40 m. Tests in ethanol or gasoline were performed with the chamber sealed and filled with dry N_2, while unlubricated tests were performed in laboratory air. Two speeds were used, 50 and 100 Hz, giving average speeds of 0.02-0.04 m/s. Loads of 2 N and 5 N were applied, giving average Hertzian contact pressures of 0.86 and 1.17 GPa and peak Hertzian contact pressures of 1.29 and 1.75 Gpa, respectively. Typical conditions were 50 Hz and 2 N.

Figure 6 on page 32 plots friction for three coated or uncoated flat materials worn against uncoated balls in two fluids, plus the unlubricated dry condition. These tests were performed at 50 Hz speed and 2 N load. Bare steel on steel gave a typically high friction value. Ethanol and gasoline provided lubrication in all cases compared to air. Gasoline lubricated bare steel better than ethanol, but coating the flat with an NFC reduced the ethanol friction to that of gasoline. Figure 7 on page 33 shows the wear rates measured from these experiments; note the logarithmic scale. The friction value is given beside each data point. While both ball wear and flat wear

were measured, the values reported were material removal from the flat, for reasons described below. Wear rates for tests of NFC-coated flats versus steel balls in ethanol and gasoline were essentially zero because the wear scars could not be found. No damage to either the ball or the flat could be identified in those cases. For uncoated steel, lubrication decreased both the wear rate and friction relative to tests in air, as expected. Friction of NFC coatings against uncoated balls in air was relatively high, perhaps due to moisture. The wear rates in air corresponded to the friction coefficients between NFC2 and NFC6. For those NFC tests in air, the wear rates of the steel balls were approximately two orders of magnitude lower than the wear rates of the coated flats.

The wear volumes were measured from 3-D optical surface profiles, such as those shown in Figure 8 on page 34. Each of the three images consists of a top-down view of the surface, covering an area given at the lower right, for example 809 x 613 μm in the case of Figure 8a. Below each image is a color scale from dark to light, with a range (in μm) giving the heights of the deepest and highest points in the image. The height value of 0 μm corresponds approximately to the plane of each image. Figure 8a shows the scar on the uncoated flat after wear against an uncoated ball in laboratory air. There is evidence of adhesion and plasticity, and so much material was removed that the width of the final scar is larger than the stroke length. In Figure 8b presents the scar from an uncoated steel flat worn against steel in ethanol. The wear scar was much smaller, with a width of approximately 100 μm, and it showed signs of material pushout, debris re-adhesion, or some other form of buildup around the edge of the scar. Figure 8c shows the scar on an NFC2-coated flat worn against steel in air. The scar was approximately the same size as that in Figure 8b, but the wear surface was polished, and no buildup was seen.

Experiments to determine the speed and load sensitivity of the coatings were performed in ethanol. Figure 9 on page 35 plots friction versus severity for bare 440C, NFC2, and NFC6 flats worn against steel in ethanol under dry nitrogen. Bare steel gave the highest friction at the low frequency of 50 Hz, especially at the low load of 2 N. At high frequency and low load, all three materials displayed the same friction within the experimental error. The friction values from NFC2 and NFC6 were the same and did not depend significantly on load or speed. Figure 10 on page 36 gives both wear rate and friction versus severity for the case of uncoated steel against steel in ethanol. The friction data are reproduced from Figure 9. The wear rate is somewhat, but not strongly, correlated to the friction and is only a weak function of severity for these ethanol-lubricated tests.

As noted above, the wear volume used to calculate the wear rate was the flat wear. This convention was adopted because the balls tested against bare steel in ethanol and gasoline had a bump of added material approximately 0.5-μm thick, rather than a hole of removed material. Initial theories as to the nature of these bumps were that (1) they were a real tribofilm added to the ball through oxidation, polymerization, and debris accumulation, or (2) they were a thin but optically active layer which was changing the phase of the light so as to appear thick to the 3-D surface profiling instrument, whose operating principle is light interferometry. Ultrasonic cleaning of the ball in xylene did not remove the bumps. To eliminate (2) as a possibility, one of the balls was sputter coated with a layer of gold approximately 50 Å thick to render the profiled surface opaque. The bump was still present in surface profiles collected afterwards. Figure 11 on page 37 shows four views of that data set, which was from a ball worn against uncoated steel in ethanol at 50 Hz and 2 N load. Figure 11a shows the top view of the ball, with the curvature visible as darkening outwards from the center. The bump is visible as the light patch in the

center. Figure 11b shows that data as viewed from the side, to illustrate the 3-D shape of the sample. The same color scale is used in Figures 11a and 11b. To clarify the surface relief of the bump of added material relative to the ball, MicroXAM was used to mathematically subtract the spherical curvature from the 3-D height data set, resulting in the top view image shown in Figure 11c. Figure 11d shows that new image as viewed from the side. Figures 11c and 11d clearly show that even after coating the surface with an opaque material, the bump is still detected as a raised area averaging approximately 0.5 μm above the surface of the sphere (appearing in Figures 11c and 11d as a plane).

To illustrate the performance of the Fretting Tester's data-collection capabilities, Figure 12 on page 38 shows plots of friction from a typical reciprocating test. This test was an NFC2-coated flat worn against a steel ball in ethanol at 50 Hz and 5 N load. Figure 12a shows average friction as a function of cycle number throughout the test. The average friction numbers reported in the rest of this work are averages of data from plots like Figure 12a. In this case, the friction was stable at 0.10, a value typical of the boundary lubrication regime. Figure 12b shows frictional force as a function of the relative position of the counterface and the flat. Three cycles from approximately cycle 50,000 are shown, and the direction of time in the force versus position loop is clockwise. A 200-μm track length was observable as the range of values on the position axis. The force loop showed a nearly square-wave force response, with some ringing overlaid as motion began in each direction. This ringing was a common observation and was probably caused by the resonant frequency of either the counterface mount or the sample cup mount.

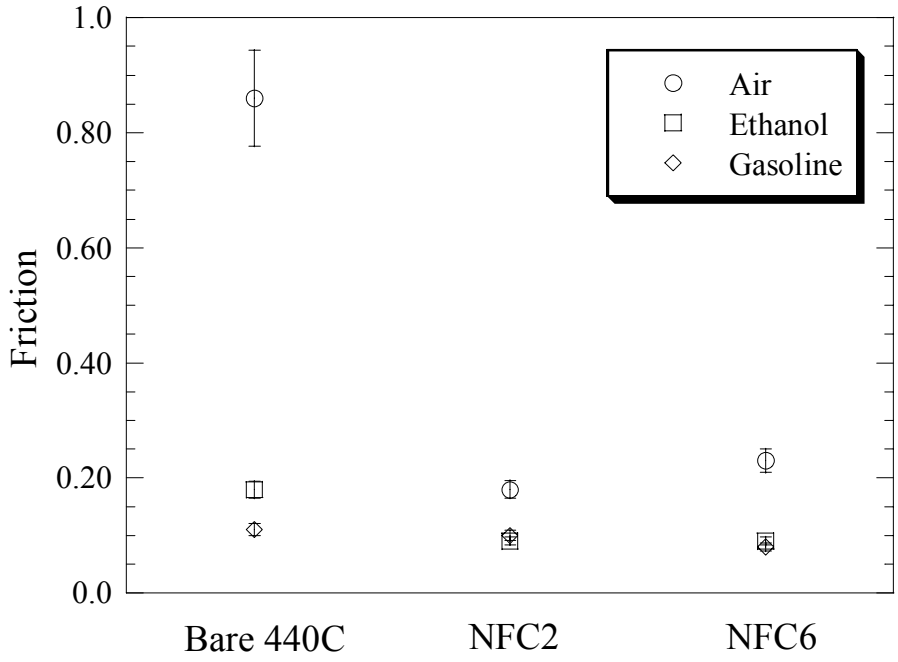

Figure 6. Friction measured for three coated or uncoated flat materials worn against uncoated 440C balls in two fluids plus air. The reciprocating tests used a track length of 200 μm and a duration of 100,000 cycles.

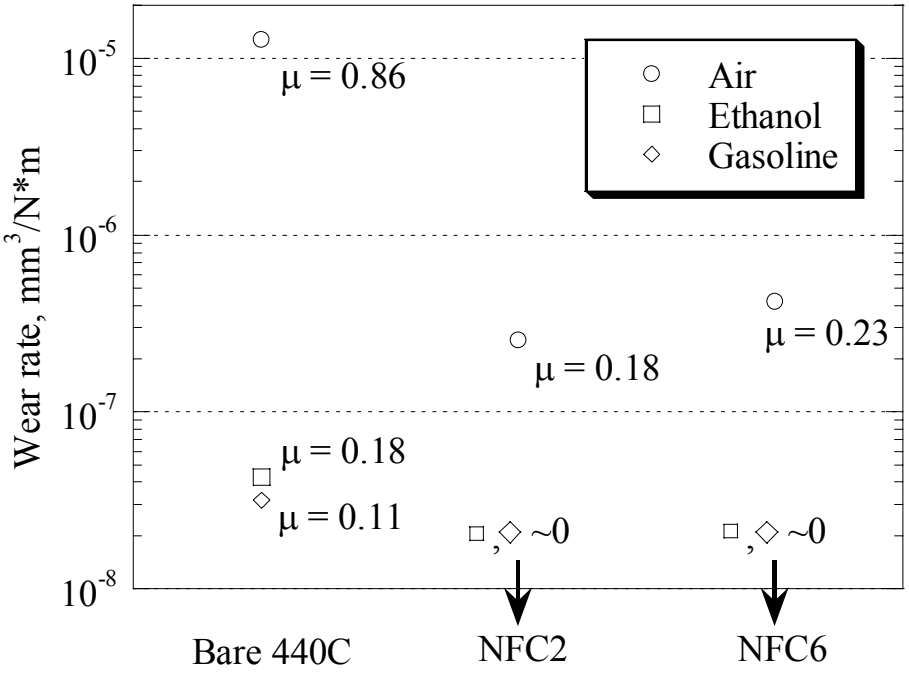

Figure 7. Wear rates for three coated or uncoated flat materials worn against uncoated 440C balls in two fluids plus air. Note the logarithmic vertical scale. The values reported are material removal from the flat.

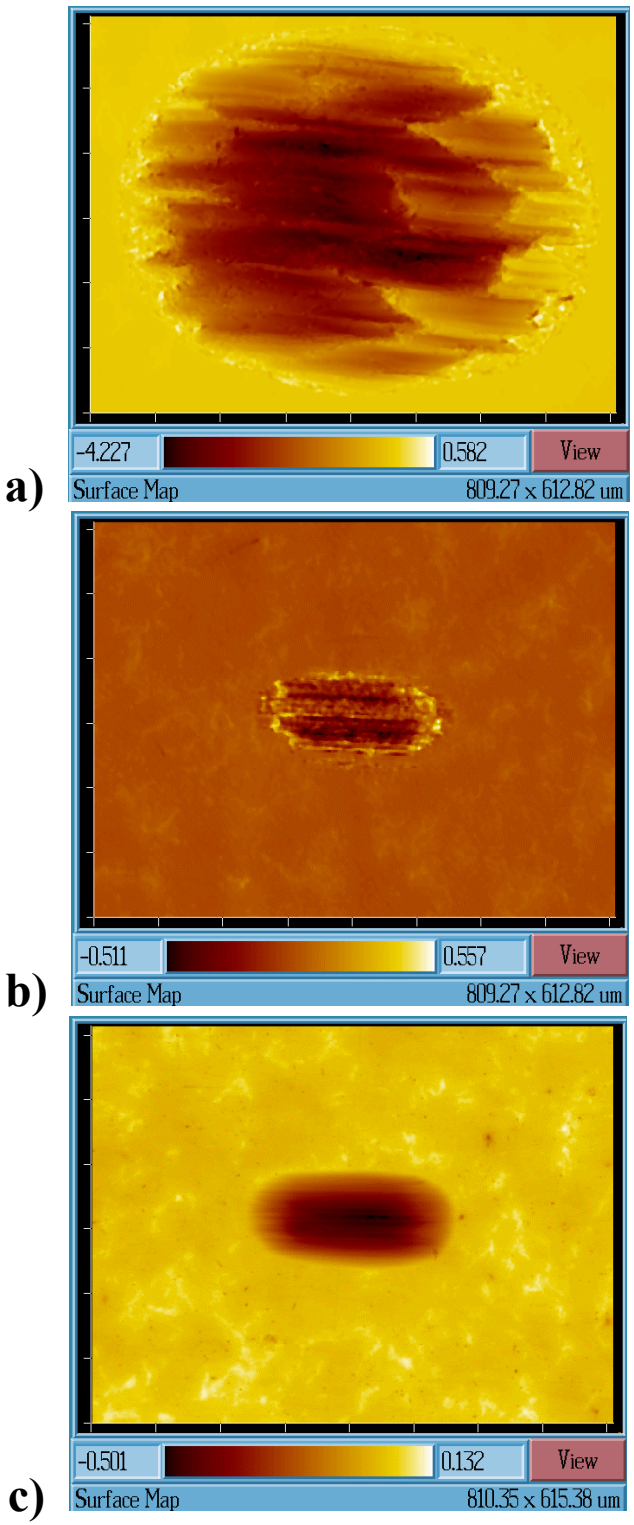

Figure 8. 3-D optical surface profiles of wear scars formed on flats in reciprocating tests. Under each image, the height scale from dark to light colors is given in μm, while the lateral scale is given at the lower right. An uncoated 440C steel flat worn against an uncoated 440C ball in air (unlubricated) is shown in (a). In (b), steel was worn on steel in ethanol. In (c), the steel flat was coated with NFC2 and worn against an uncoated ball in air.

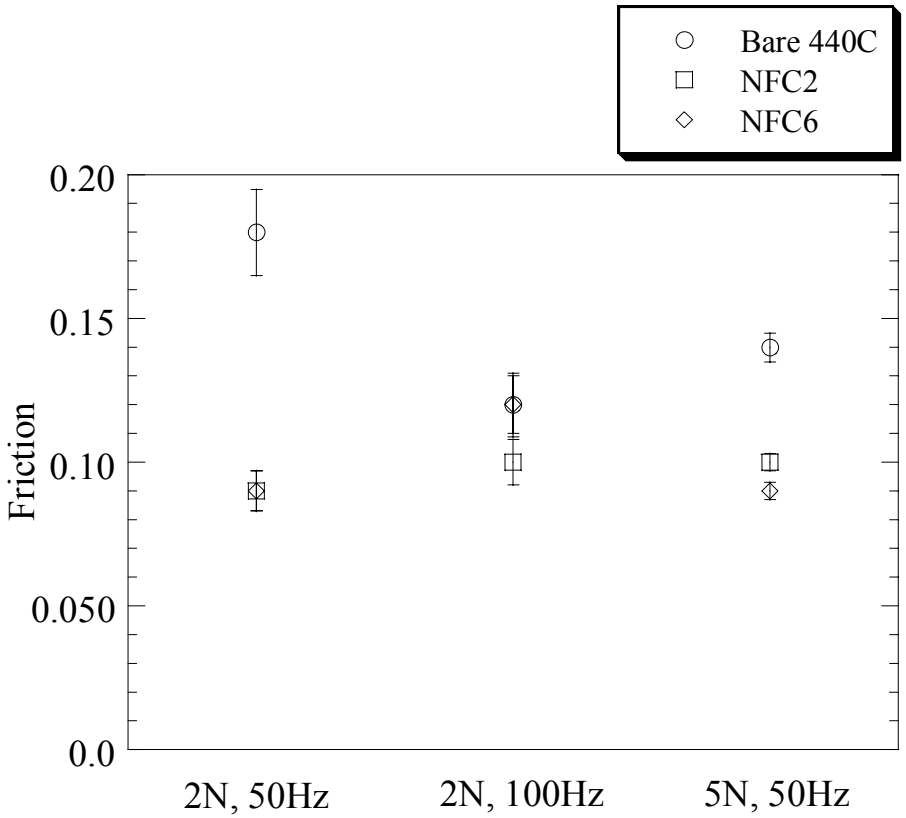

Figure 9. Friction coefficient versus material and severity (load and speed) for several flat materials in reciprocating tests against 440C balls in ethanol.

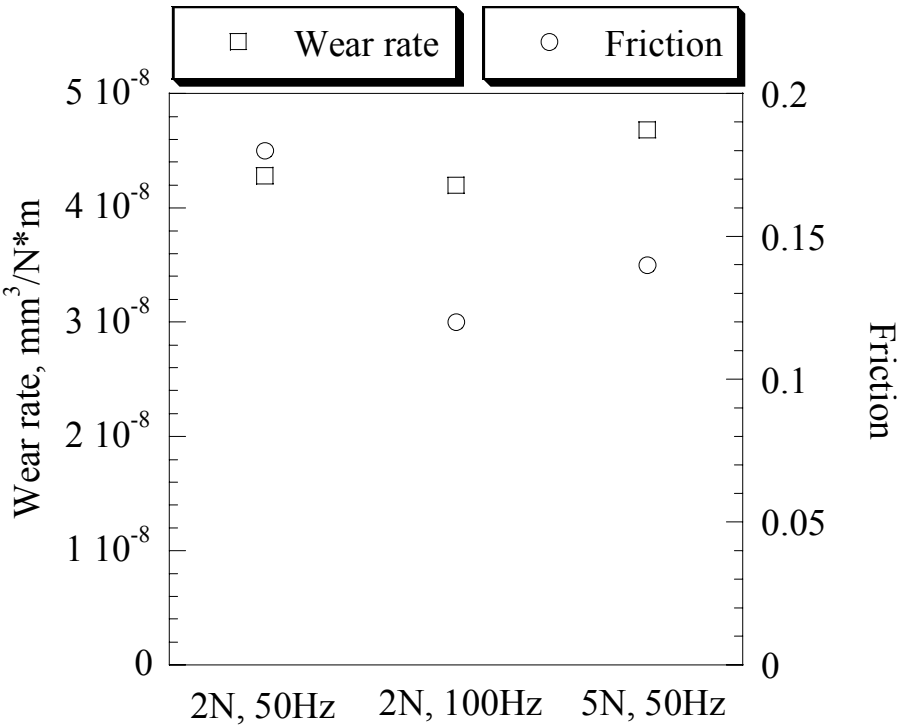

Figure 10. Wear rate and friction versus severity for uncoated steel worn against steel in ethanol. The vertical scale is not logarithmic in this case.

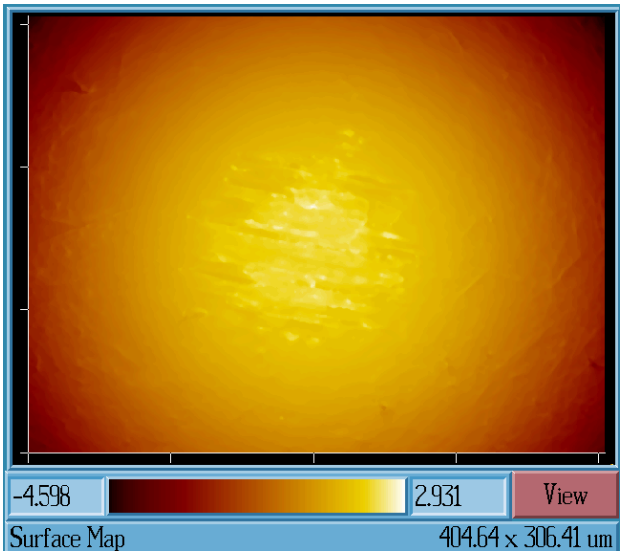

a) above

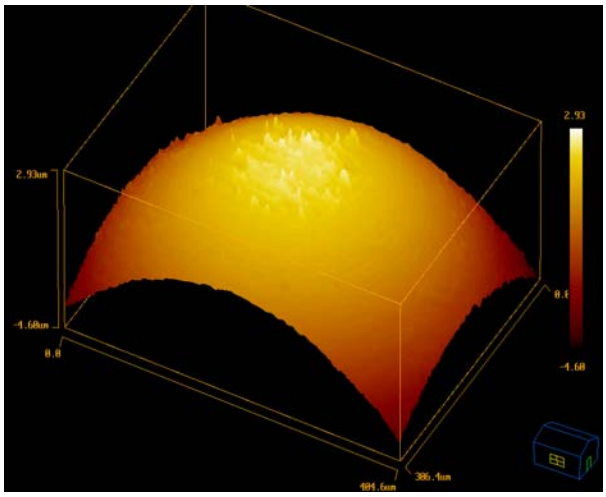

b) above

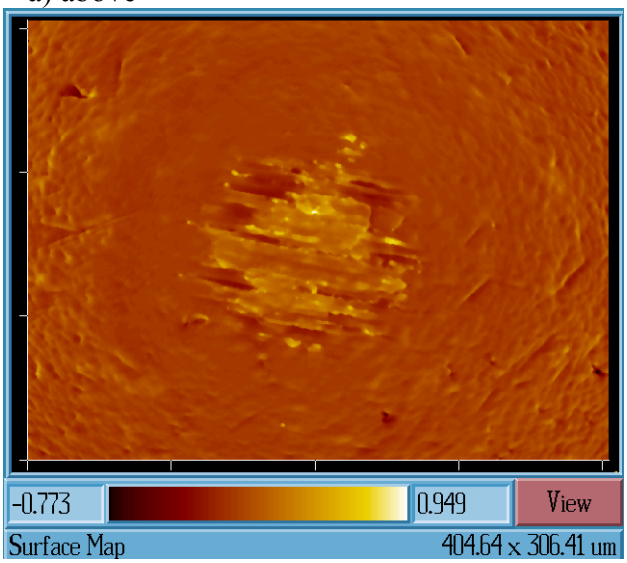

c) above

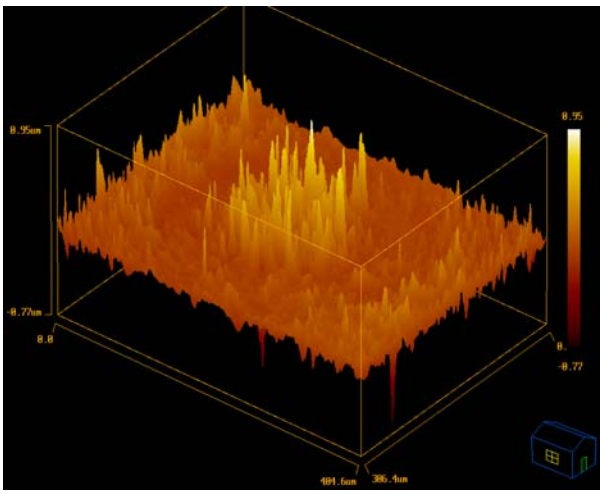

d) above

Figure 11. 3-D surface profiles of a wear scar formed on a 440C ball during a reciprocating test against steel in ethanol. Figure 11(a) shows the scar in plan view with the height scale from dark to light shown at the bottom of the image. Image (b) shows the same data set viewed from the side. Image (c) is a plan view of the scar after mathematically subtracting the spherical curvature (note the new height scale). Image (d) is that data set viewed from the side.

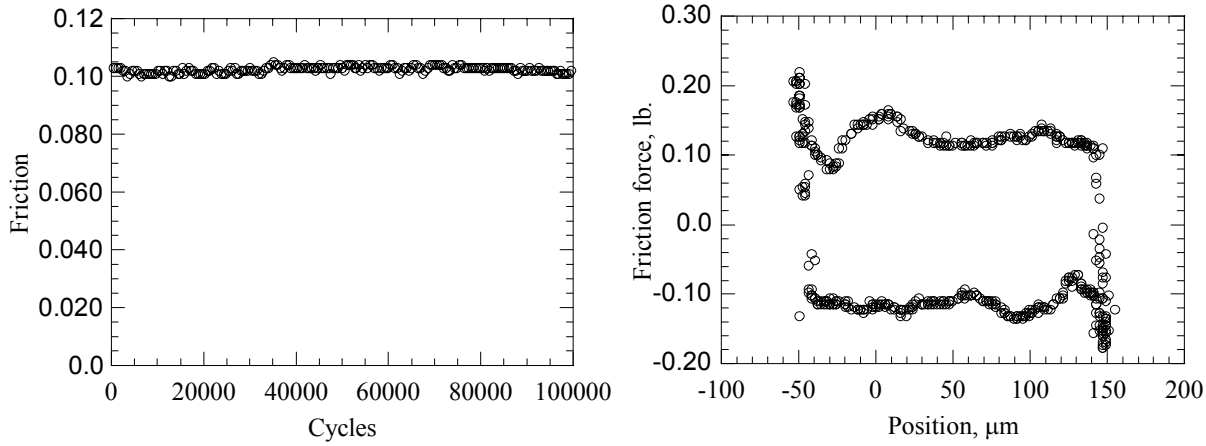

Figure 12. Friction plots from a typical reciprocating test. Friction versus cycle number is shown in 12a while in 12b friction force versus position is shown for three cycles in the middle of the test.

C. Short-Duration Reciprocating Tests with Standard Fuels

Having established that the NFC coatings were effective at reducing wear when lubricated by fuels in conditions simulating the operating parameters of a fuel injector, a comprehensive study was performed to compare the fuel-lubricated wear behavior of NFCs with three commercial DLC coatings. For these tests, the stroke length was increased from 200 μm to 1 mm, but the duration was held constant at 100,000 cycles to keep the total testing time down. The five plots in Figures 13 through 17 on pages 42 through 46 show the friction and wear results for dry (unlubricated), ethanol, E85, M85, and gasoline in the sample cup, respectively. In each of these plots, the friction is given as a black bar with error and is read on the left Y-axis; the wear rates are read off the right Y-axis. The wear rates are presented as a red and blue bar with a total height corresponding to the total wear rate. The red fraction of the bar gives the wear rate of the flat, while the blue part of the bar gives the wear rate of the coated injector. The X-axis is the coating applied to the injector tip (the flats were uncoated). The trends from coating to coating within the data for a particular lubricant shown in Figures 13-17 will be discussed below, followed by a reexamination of the data in terms of fuel-to-fuel variations for each coating.

In the case of unlubricated contact, the uncoated case forced the wear rate axis in Figure 13 to a scale two orders of magnitude larger than those in Figures 14-17. No coating achieved low friction in lab air without lubricant. Note that the wear rate of Commercial DLC2 was over half that of uncoated steel, indicating that it would be a poor choice for applications where it might be run dry. Even Commercial DLC3 showed a wear rate several times that of the worst lubricated wear, which was for uncoated parts lubricated by M85 fuel. By comparison, wear

rates for NFC2, NFC6, and Commercial DLC1 were several orders of magnitude lower than the other surface treatments. NFC6 outperformed Commercial DLC1 by 15%.

For wear in ethanol (Figure 14), included in this study as a well-characterized and universal lubricant for comparisons, the friction and wear data did not vary between coatings as much as in the unlubricated case. The lowest friction values were achieved by NFC2, NFC6, and Commercial DLC1, while Commercial DLC2 and Commercial DLC3 gave friction equal to or greater than that of uncoated steel. The wear rate for Commercial DLC2 was the highest, exceeding even uncoated steel. The lowest wear rates were again achieved by NFC2, NFC6, and Commercial DLC1, with NFC 6 outperforming Commercial DLC1 by 24%. These values represented an improvement of approximately a factor of 10 compared to uncoated surfaces.

Friction and wear rates in E85 fuel (Figure 15) showed NFC2, NFC6, and commercial DLC1 with typically low friction values, but Commercial DLC1 suffered a wear rate more than double that of the NFCs. Commercial DLC2 showed an anomalously high wear rate, far exceeding that of the uncoated surface, and it would obviously be a poor choice for alternative fuel applications. The results for M85 fuel shown (Figure 16) were similar. NFC2, NFC6, and Commercial DLC1 had the lowest friction, but Commercial DLC1 had a higher wear rate; Commercial DLC3 showed a surprisingly low wear rate (25% better than that of NFC2 in this fuel) considering its high friction.

The results for wear in regular gasoline are given in Figure 17. NFC2 provided the best friction, with the three commercial DLCs giving values almost as low. The lowest friction of the commercial DLCs was number 2, which unfortunately again produced an anomalously high wear rate. The lowest wear rate of the group was achieved by NFC2, followed by Commercial DLC3;

wear rates in gasoline were generally proportional to friction with the exception of the uncoated case and Commercial DLC2.

The data from Figures 13 through 17 are presented in a different format in Figures 18 through 20 on pages 47 through 49. In these figures, one surface treatment is presented per plot and the lubricant is given along the X-axis to reveal variations with chemistry.

Figure 18 gives friction and wear rate versus lubricant for uncoated injectors. The coefficient of friction of 1.32 for unlubricated, uncoated materials exceeded the Y-scale; of the others, gasoline and E85 fuel caused the highest friction and M85 the lowest. As noted previously, however, uncoated surfaces worn in M85 suffered a higher wear rate than they did in other liquids. The friction scale from zero to 0.5 was held constant for Figures 18-20; the wear rate axis scale could not be kept constant due to the extreme behavior of the dry tests.

In tests of NFC2 in various liquids shown in Figure 19, all friction coefficients were decreased compared to tests of uncoated materials in the same fluids. The greatest friction improvements were seen in E85 (67% reduction) and gasoline (55% reduction) fuels. Wear rates were also improved; note that the vertical axis was three orders of magnitude smaller for the NFC2 plot compared to the uncoated plot. Ignoring the dry tests, the range of total wear rates for NFC2 was 1.2-2.2x10^{-8} mm^3/N·m, while the total wear rates for uncoated samples was 4.3x10^{-8} to 6.4x10^{-7} mm^3/N·m. Again, M85 fuel was the most aggressive environment in terms of wear. NFC6 performed similarly to NFC2 but with slightly elevated friction coefficients and wear rates, except when lubricated by ethanol.

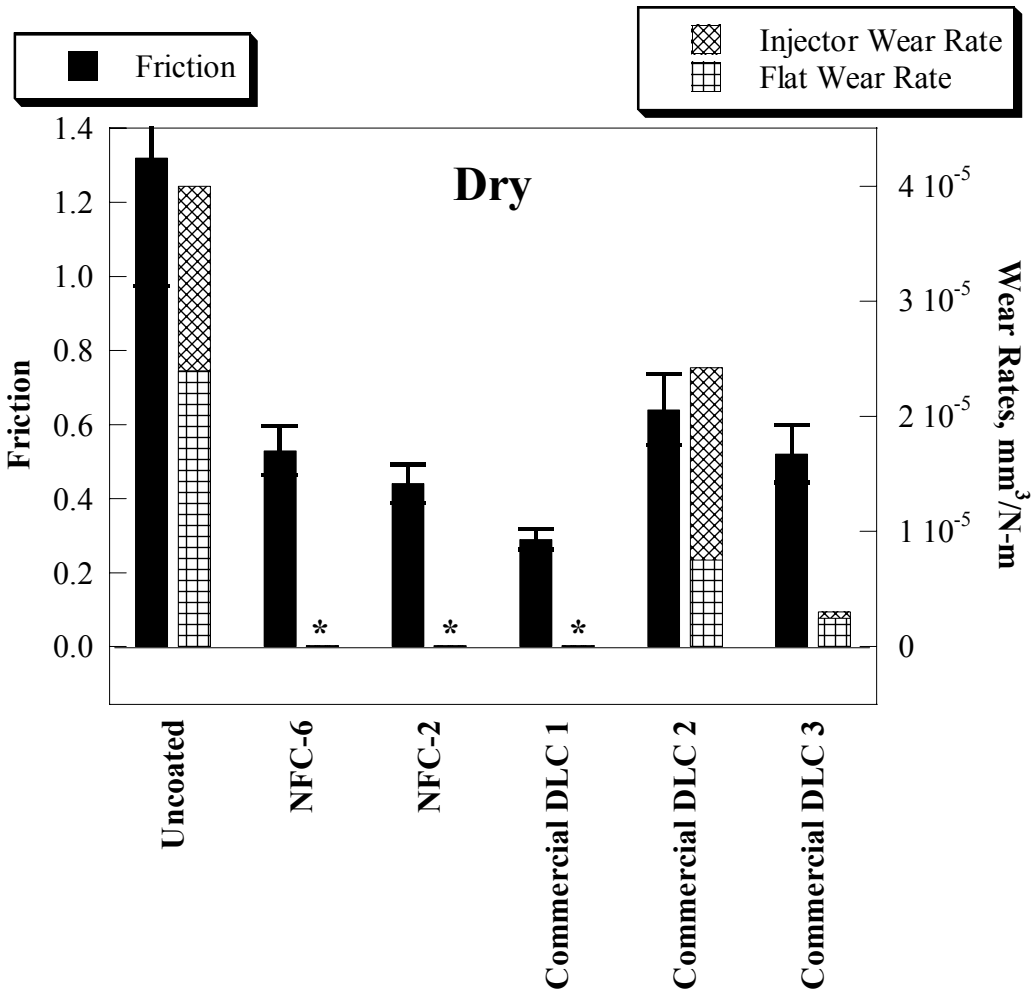

Figure 13. Friction and wear rates for several injector coatings in reciprocating wear without lubrication. Friction is shown in black and corresponds to the Y-axis on the left. For the right Y axis, the horizontally patterned portion of the column represents wear on the uncoated steel flat, while the diagonally patterned portion gives wear of the coated injector. The asterisks [*] indicate near-zero wear.

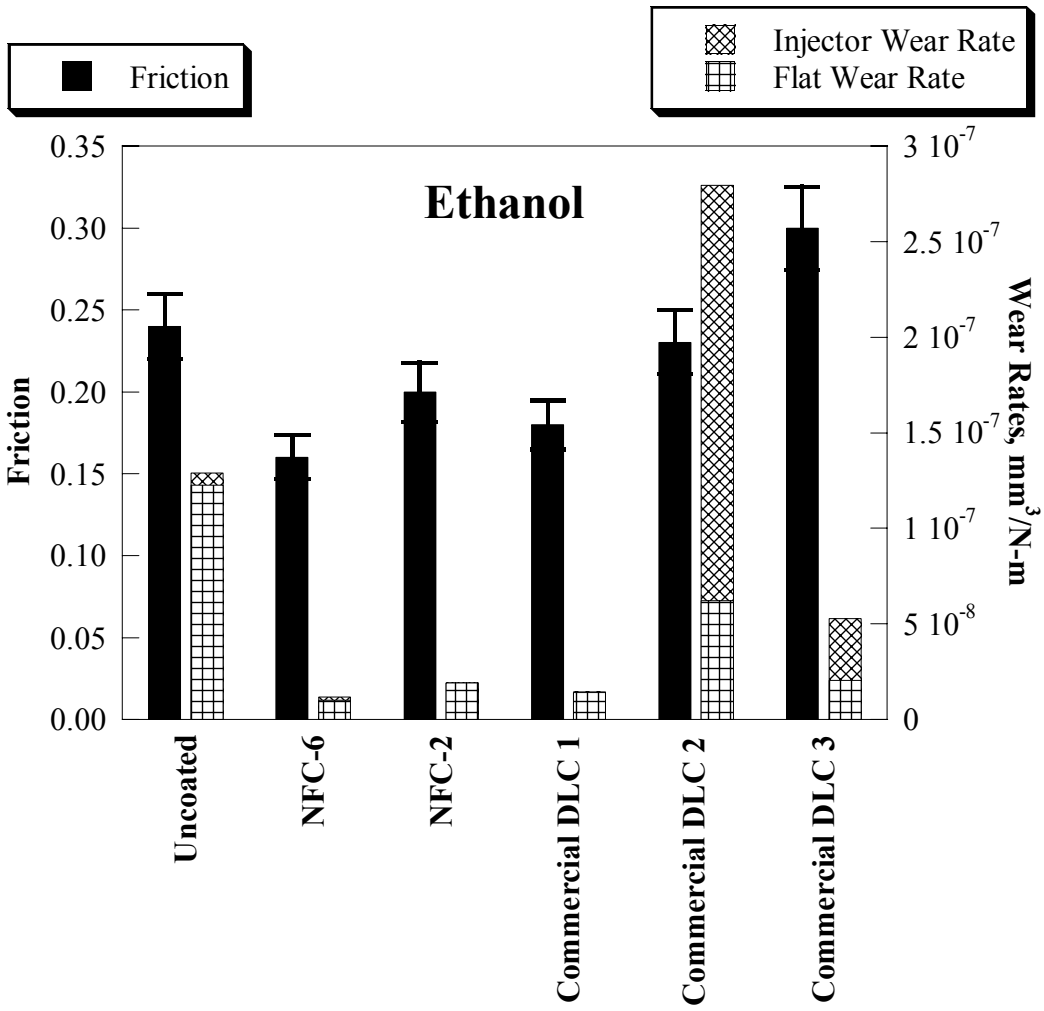

Figure 14. Friction and wear rates for several injector coatings in reciprocating wear in ethanol. Friction is shown in black and corresponds to the Y axis on the left. For the right Y-axis, the horizontally patterned portion of the column represents wear on the uncoated steel flat, while the diagonally patterned portion gives wear of the coated injector.

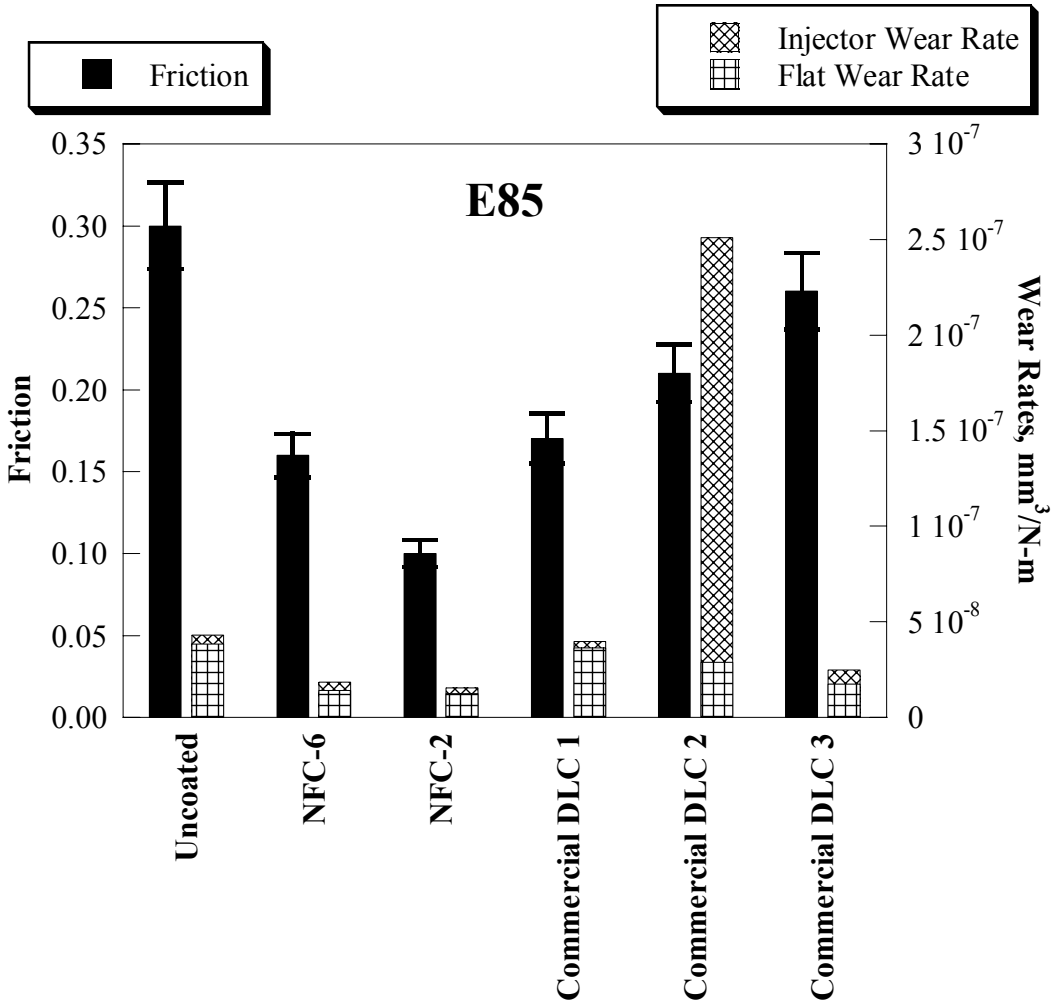

Figure 15. Friction and wear rates for several injector coatings in reciprocating wear in E85 fuel. Friction is shown in black and corresponds to the Y-axis on the left. For the right Y-axis, the horizontally patterned portion of the column represents wear on the uncoated steel flat, while the diagonally patterned portion gives wear of the coated injector.

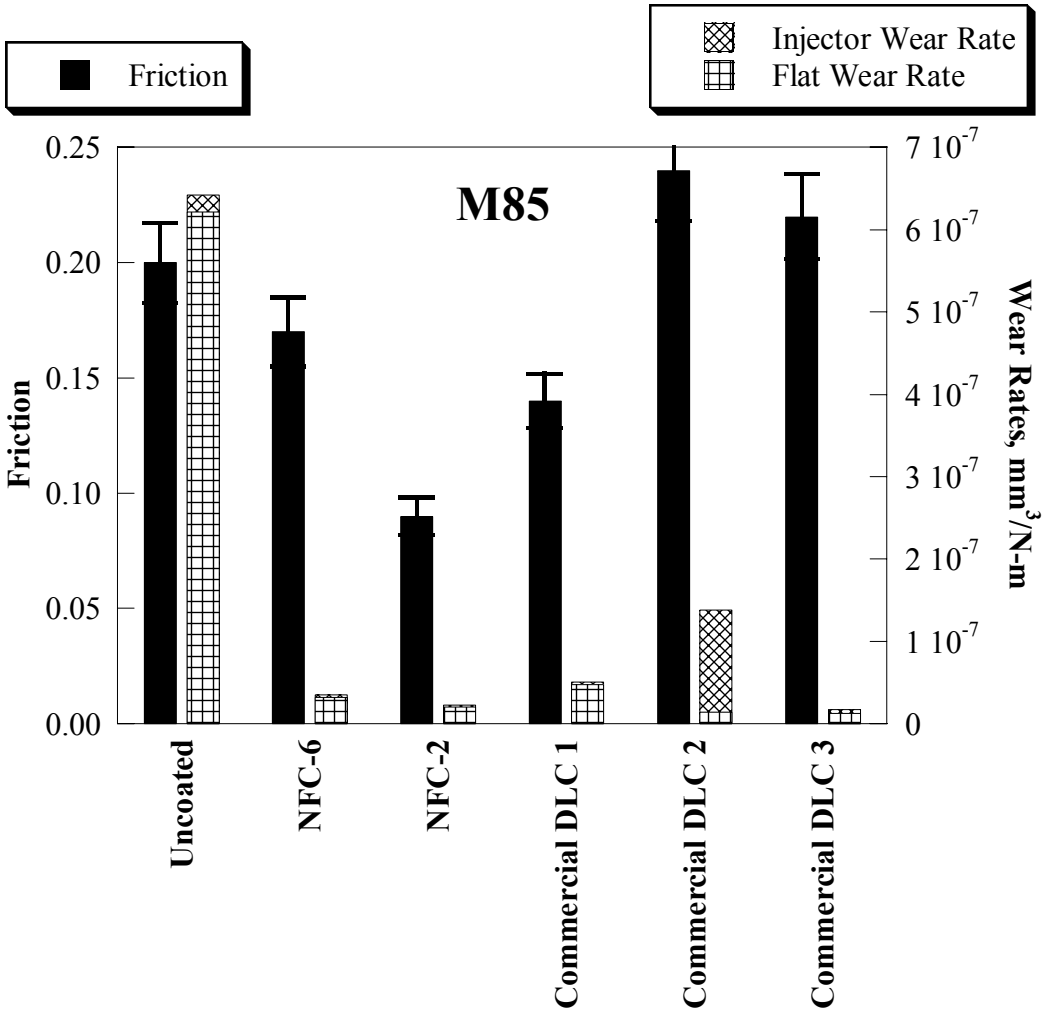

Figure 16. Friction and wear rates are shown for several injector coatings in reciprocating wear in M85 fuel. Friction is shown in black and corresponds to the Y-axis on the left. For the right Y-axis, the horizontally patterned portion of the column represents wear on the uncoated steel flat, while the diagonally patterned portion gives wear of the coated injector.

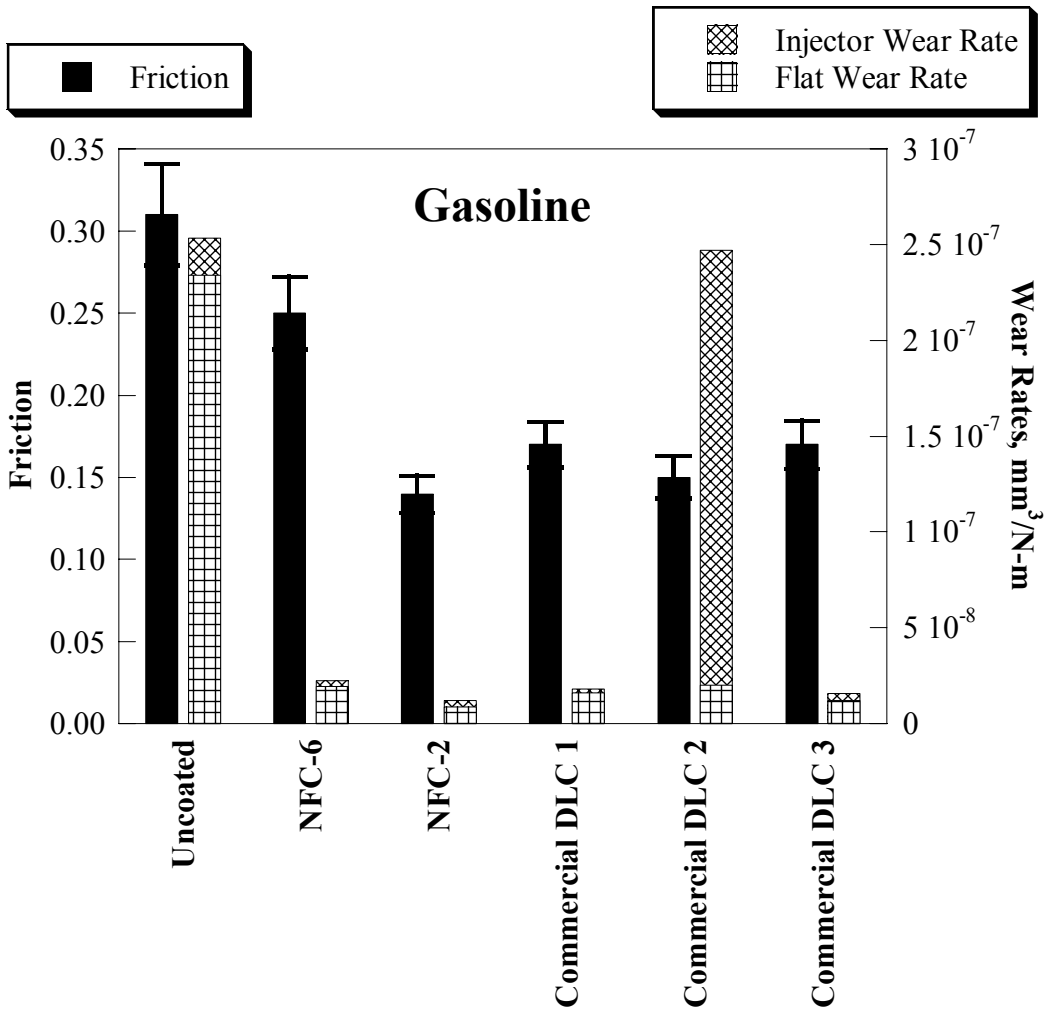

Figure 17. Friction and wear rates for several injector coatings in reciprocating wear in gasoline. Friction is shown in black and corresponds to the Y-axis on the left. For the right Y-axis, the horizontally patterned portion of the column represents wear on the uncoated steel flat, while the diagonally patterned portion gives wear of the coated injector.

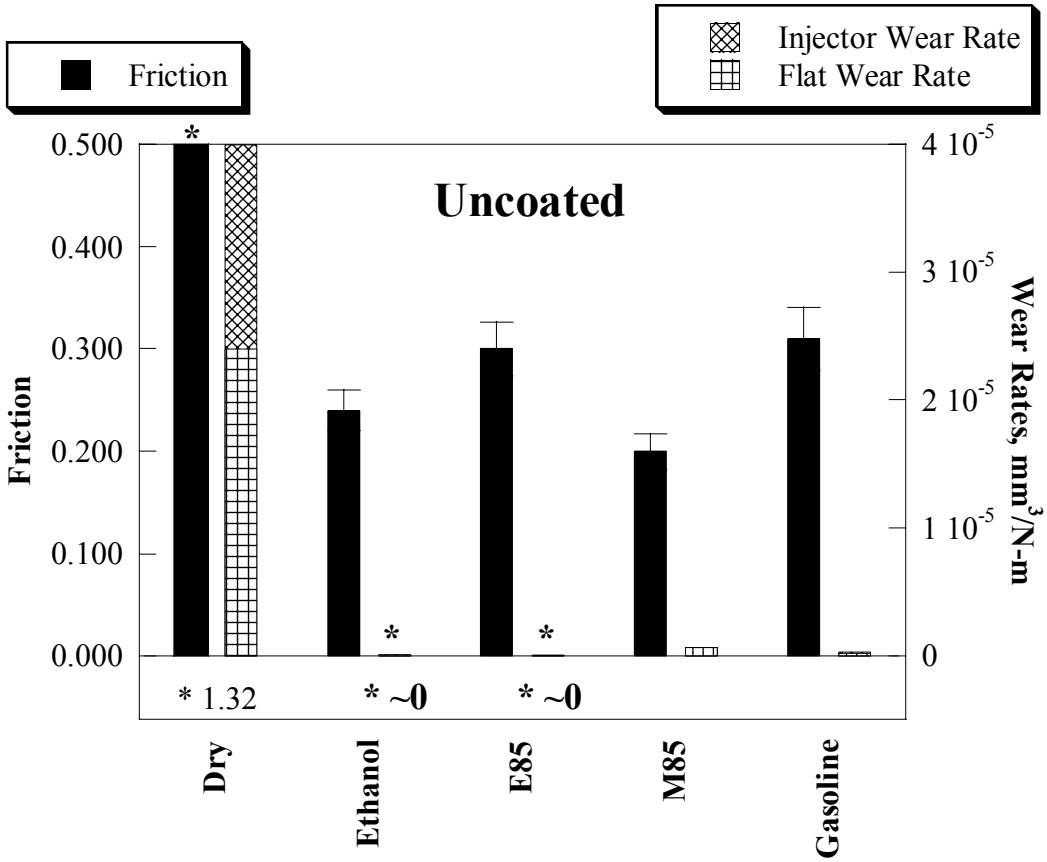

Figure 18. Friction and wear rates for uncoated injectors in reciprocating wear in several liquids. Friction is shown in black and corresponds to the Y-axis on the left. For the right Y-axis, the horizontally patterned portion of the column represents wear on the uncoated steel flat, while the diagonally patterned portion gives wear of the coated injector.

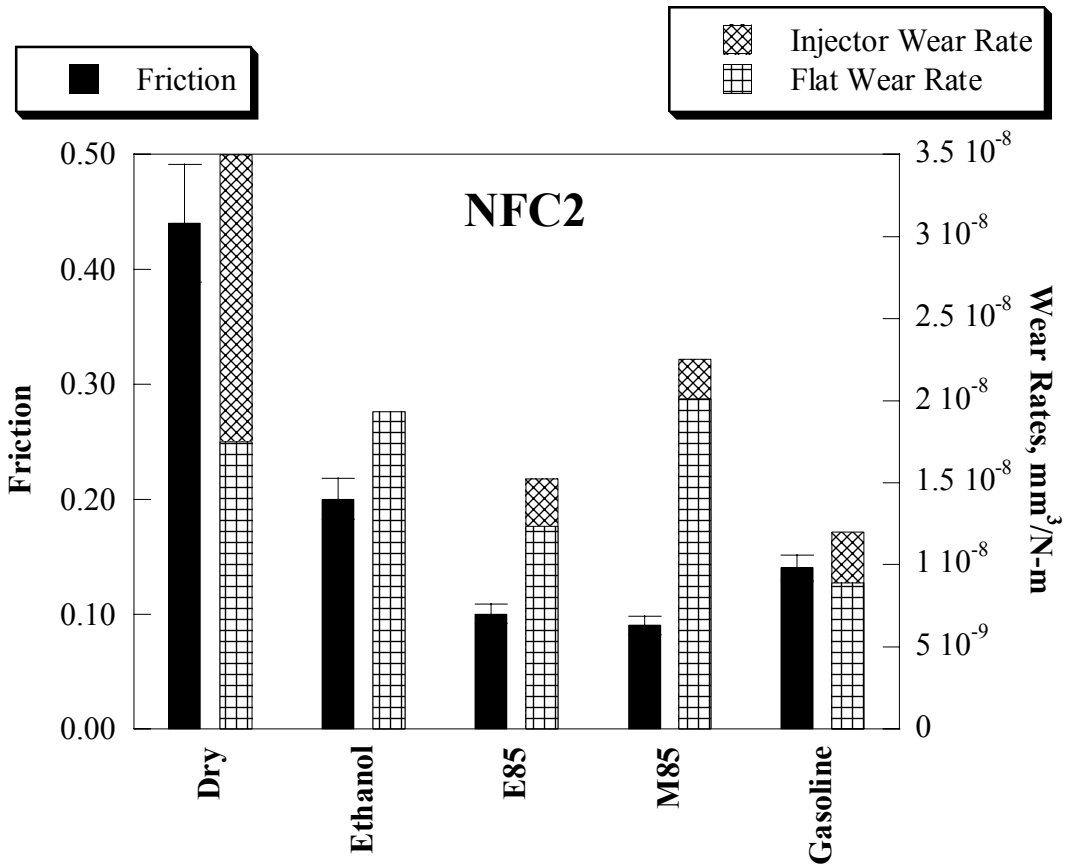

Figure 19. Friction and wear rates for NFC2-coated injectors in reciprocating wear in several liquids. Friction is shown in black and corresponds to the Y-axis on the left. For the right Y-axis, the horizontally patterned portion of the column represents wear on the uncoated steel flat, while the diagonally patterned portion gives wear of the coated injector.

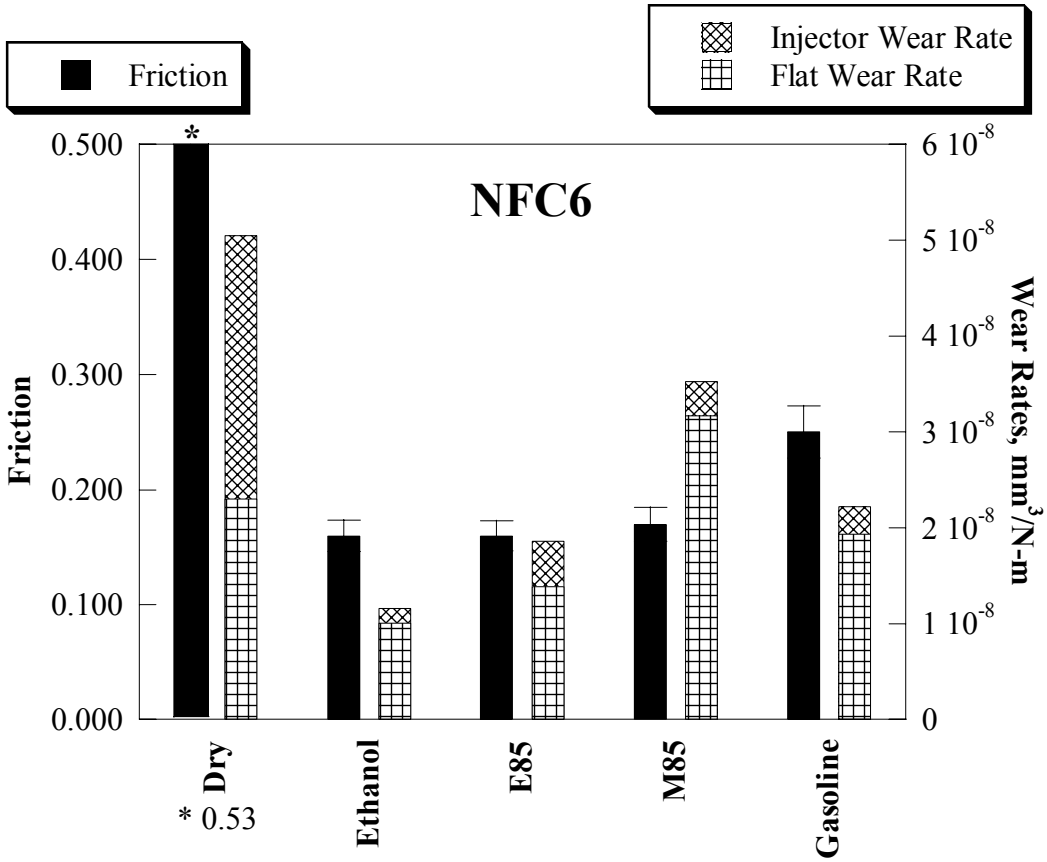

Figure 20. Friction and wear rates for NFC6-coated injectors in reciprocating wear in several liquids. Friction is shown in black and corresponds to the Y-axis on the left. For the right Y-axis, the horizontally patterned portion of the column represents wear on the uncoated steel flat, while the diagonally patterned portion gives wear of the coated injector.

D. Long-Duration Reciprocating Tests in Formulated Gasolines

After the performance of NFC-coated fuel injectors was found to be good compared to parts coated with other commercial DLCs, the reciprocating tests were used to determine the ultimate wear lifetime of the NFC coatings in regular and reformulated gasolines. This series of tests was performed for two reasons. The first reason was durability: while the short reciprocating tests indicated that the performance of the NFC coatings was good, they did not address whether this performance would last the lifetime of the part, or what would happen once it wore through. If coating removal were followed by immediate catastrophic failure of the part, extra attention would have to be paid to the design, and use of the coating might be precluded. As a result, the duration of the reciprocating tests was extended from 100,000 cycles to 1,000,000 cycles. The stroke length of 1 mm gave a total sliding distance of 2-km.

The second reason for performing this series of tests was that the coatings were to be used in SIDI engines, which will ultimately require reformulation of the North American gasoline supply when applied. Early PFI systems suffered from deposits on the injectors in much the same way that current SIDI injectors do, but efforts by the oil industry produced gasolines which were more compatible with the designs.[6] Therefore, Argonne collaborator BP Amoco plc furnished several varieties of regular gasoline and candidates for reformulated gasoline for wear testing. Table 2 on page 61 lists the gasolines tested and their characteristics. Winter and summer gasolines differ in the amount of water they contain; premium and regular gasolines have different octane numbers. The additive put into some of these gasolines was proprietary; therefore, details on its composition were not available, but it was not a compound designed for wear reduction.

Figures 21 through 24 on pages 54 through 57 show, respectively, the friction, the wear rate of the uncoated flats, the wear rate of the coated injectors, and the total wear rates in this set of tests. The tests were carried out for uncoated, NFC2-coated, and NFC6-coated injectors, and in ethanol and seven types of gasoline, which provide the two X-axes for each of the plots in Figures 21-24.

Trends in the friction data may be found by averaging the friction results for each coating over the seven gasolines used, and by averaging the friction results for each gasoline over the two NFC coatings used. Table 3 on page 61 shows the friction result for the two surface treatments averaged over the seven gasolines. The NFC coatings provide clear improvements in friction over the uncoated fuel injectors. NFC6 gives 27% lower friction, while use of NFC2 results in a friction reduction of nearly a factor of two. This has important ramifications for part longevity, such as reducing local heat buildup at the friction contact and the tendency to bind in close tolerances. Examining the other friction results, averaging the coatings for each gasoline, gives tightly grouped numbers, each of which has a large standard deviation. In other words, the major factor influencing friction is the coating, not the gasoline. Notable exceptions are ethanol and Gasoline G, which provide relatively low friction.

Similarly, trends in the wear data may be observed by averaging results for each coating over the seven gasolines and by averaging the results for each gasoline over the two NFC coatings and the uncoated material. Attention to the differences among injector wear, flat wear, and the total wear reveal additional information. Table 4 on page 61 shows the trends. Applying NFC coatings on the injectors again provided clear improvements in total wear rate and wear rate of the flats compared to the uncoated injectors. Reductions in wear ranged from an over one-third to over a factor of four. In the case of the coated injectors themselves, NFC6 provided a

wear rate very similar to that of the uncoated surface, while the NFC2 coating wore significantly faster than NFC6 and the uncoated part. Taking into account the extremely low friction provided by NFC2 in the tests, we may speculate that NFC2 is slowly sacrificing itself in order to reduce both friction and counterface wear. In contrast, NFC6 provides reductions of both friction and wear nonsacrificially. Averaging the other wear results for the coatings for each gasoline, we see trends similar to those in the friction. Wear rate averages are tightly grouped, but the averaged numbers (for different coatings) are highly variable. Gasolines A and B and ethanol produced somewhat higher wear on both flats and injectors, while Gasolines C and D lowered wear, but in general, the major factor influencing wear is the surface treatment, not the gasoline.

A wear scar from a 1,000,000-cycle lifetime test is shown in Figure 25 on page 58. This image is a top-down view of a 3-D surface profile similar to Figure 11c; like that image, the curvature of the spherical injector tip was removed from this data set to give the appearance of a plane with an indentation. The scar was from a wear test of an NFC2-coated injector worn in gasoline A. In this micrograph, the boundary between the coating and the substrate was clearly visible. The coating wore smoothly, while the areas of exposed steel and the coating next to it were rough. Only a very small amount of substrate wore off in this experiment.

Figure 26 on page 59 gives a standard optical micrograph of part of the wear track from the steel flat against which the injector of Figure 25 was worn. The scale of the image is similar to that of Figure 25; the wear scars in the images are of equal width, about 250 μm. Again, the differences between the areas worn by NFC and the areas worn by the exposed substrate were clearly visible, despite the fact that the entire sample shown was steel. Figure 27 on page 60 shows the friction trace during this test. The friction was stable throughout the first half of the test, but a sudden increase occurred at 500,000 cycles. This was followed by a less rapid drop;

during the second half of the test the noise in the friction was much larger. Repeatedly, sudden small increases in friction were followed with slower decreases. We interpret this behavior (and the morphological data in Figures 25 and 26) as follows. During the first half of the test, NFC was rubbing against steel, creating a smooth wear surface and stable friction. Halfway through the test, the NFC wore through, allowing steel-to-steel contact. The contacting steel surfaces quickly reacted with the gasoline, perhaps forming an oxide, and this reduced the friction. Additives in gasoline may also have formed thin protective films on exposed steel surfaces wearing in the boundary-layer lubrication regime. Then, pieces of steel began to be torn off the surfaces, causing abrasive wear in the center of the scar; friction rose and fell as new steel was exposed and reacted.

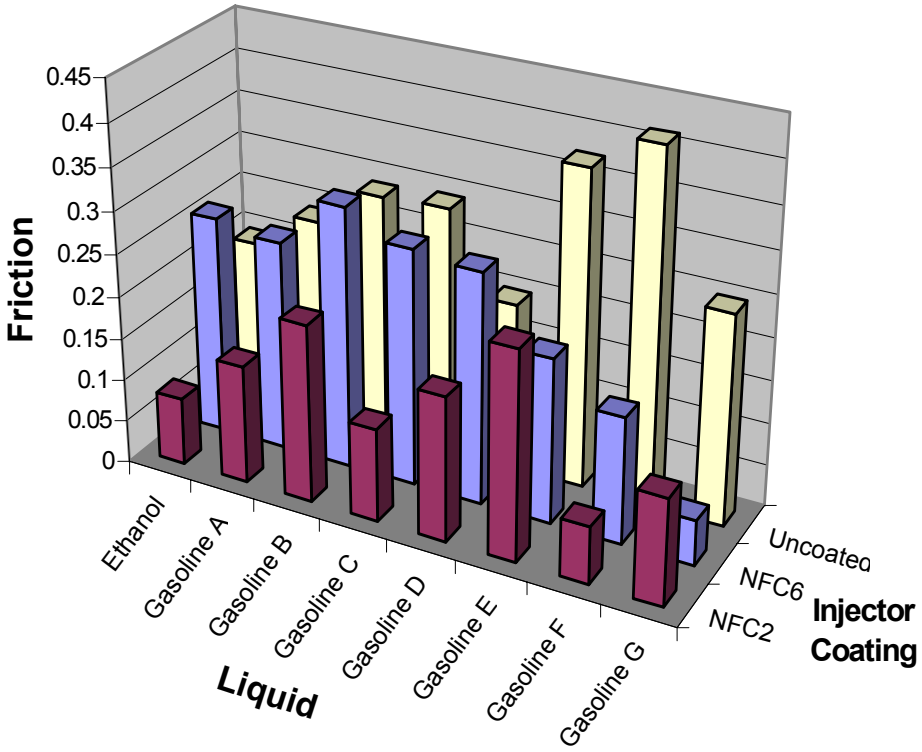

Figure 21. Friction in long-term tests for NFC-coated and uncoated fuel injectors in several gasolines.

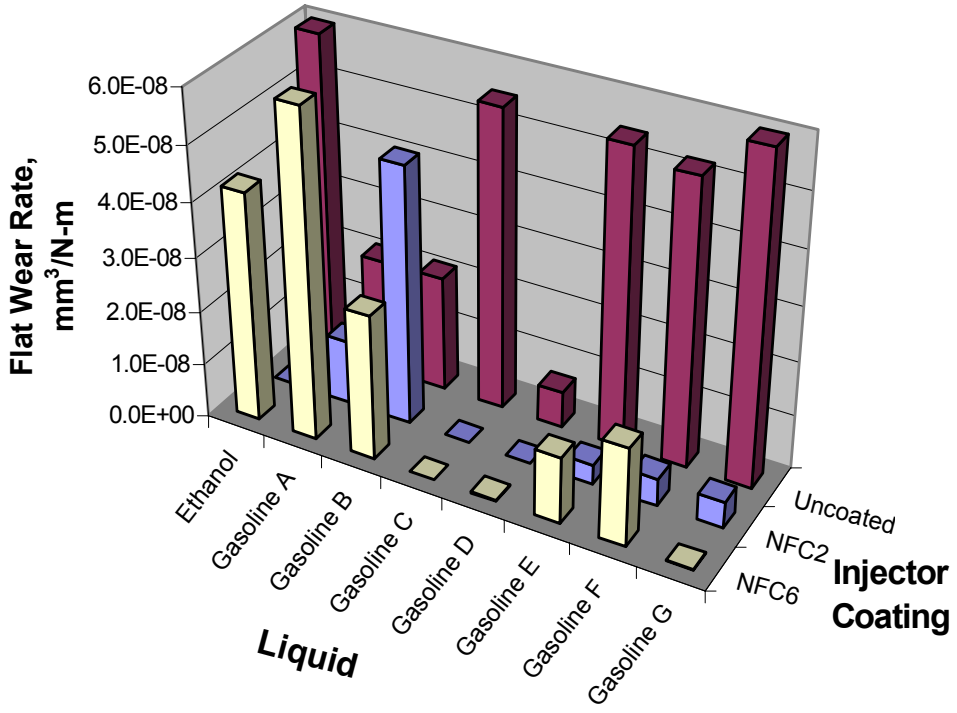

Figure 22. Wear rates of steel flats worn against NFC-coated and uncoated fuel injectors in long-term tests in several gasolines.

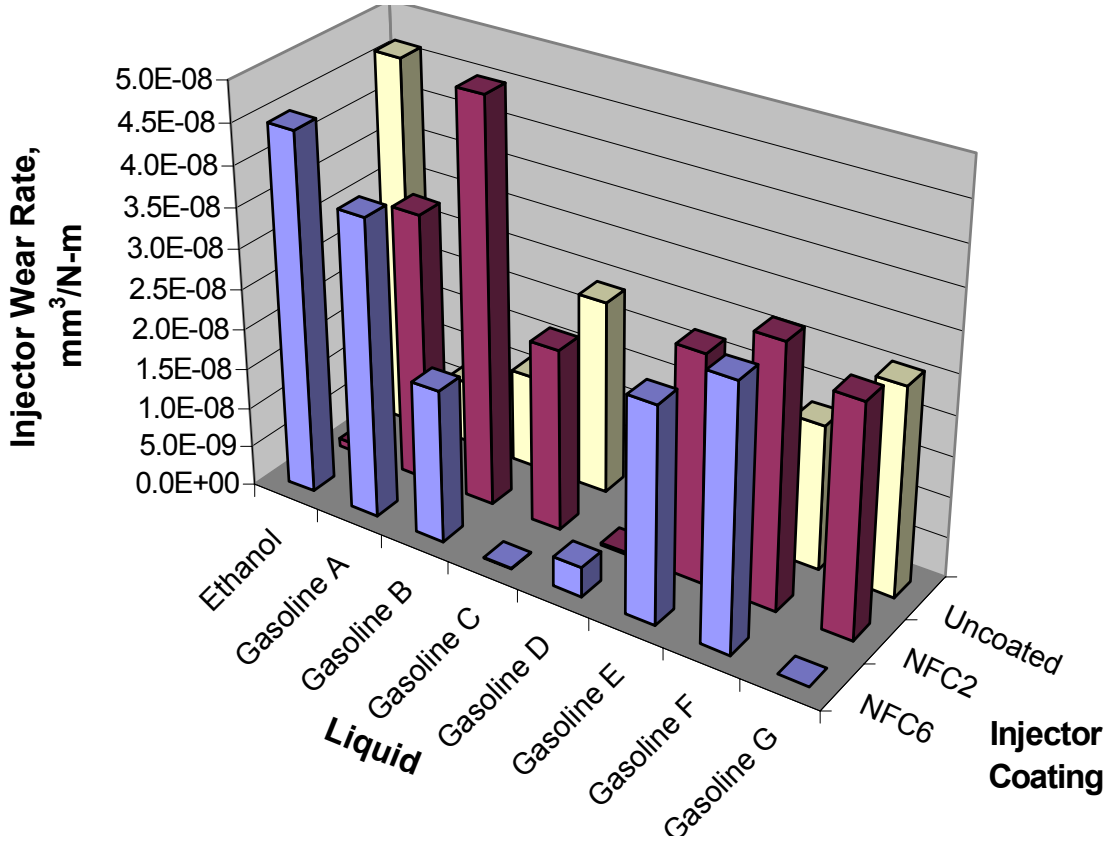

Figure 23. Wear rates of NFC-coated and uncoated fuel injectors in long-term tests in several gasolines.

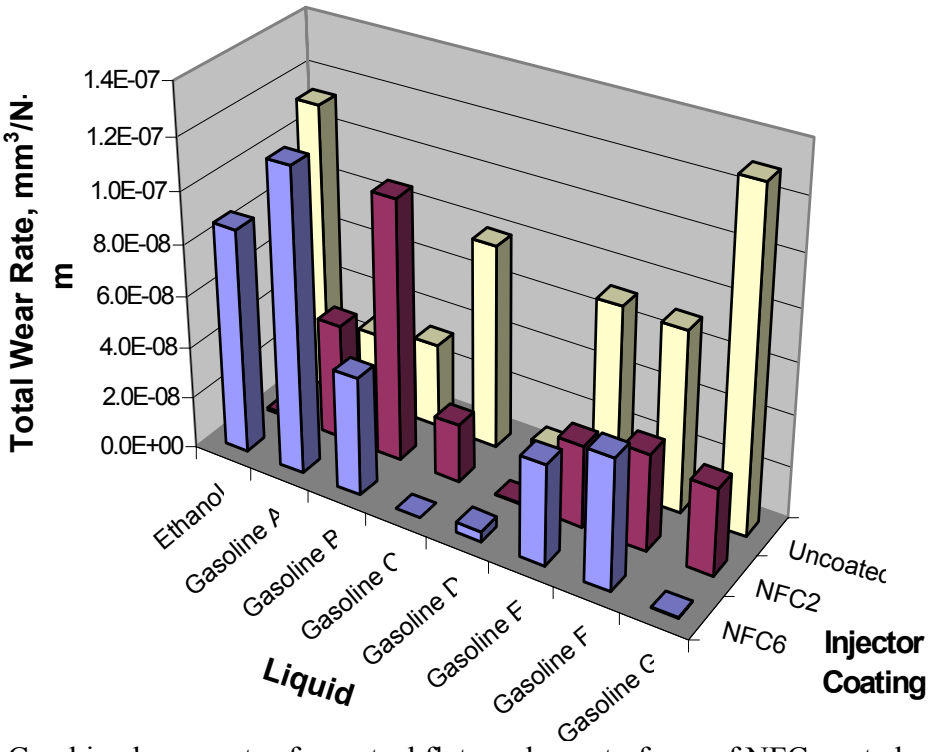

Figure 24. Combined wear rates from steel flats and counterfaces of NFC-coated and uncoated fuel injectors worn in long-term tests in several gasolines.

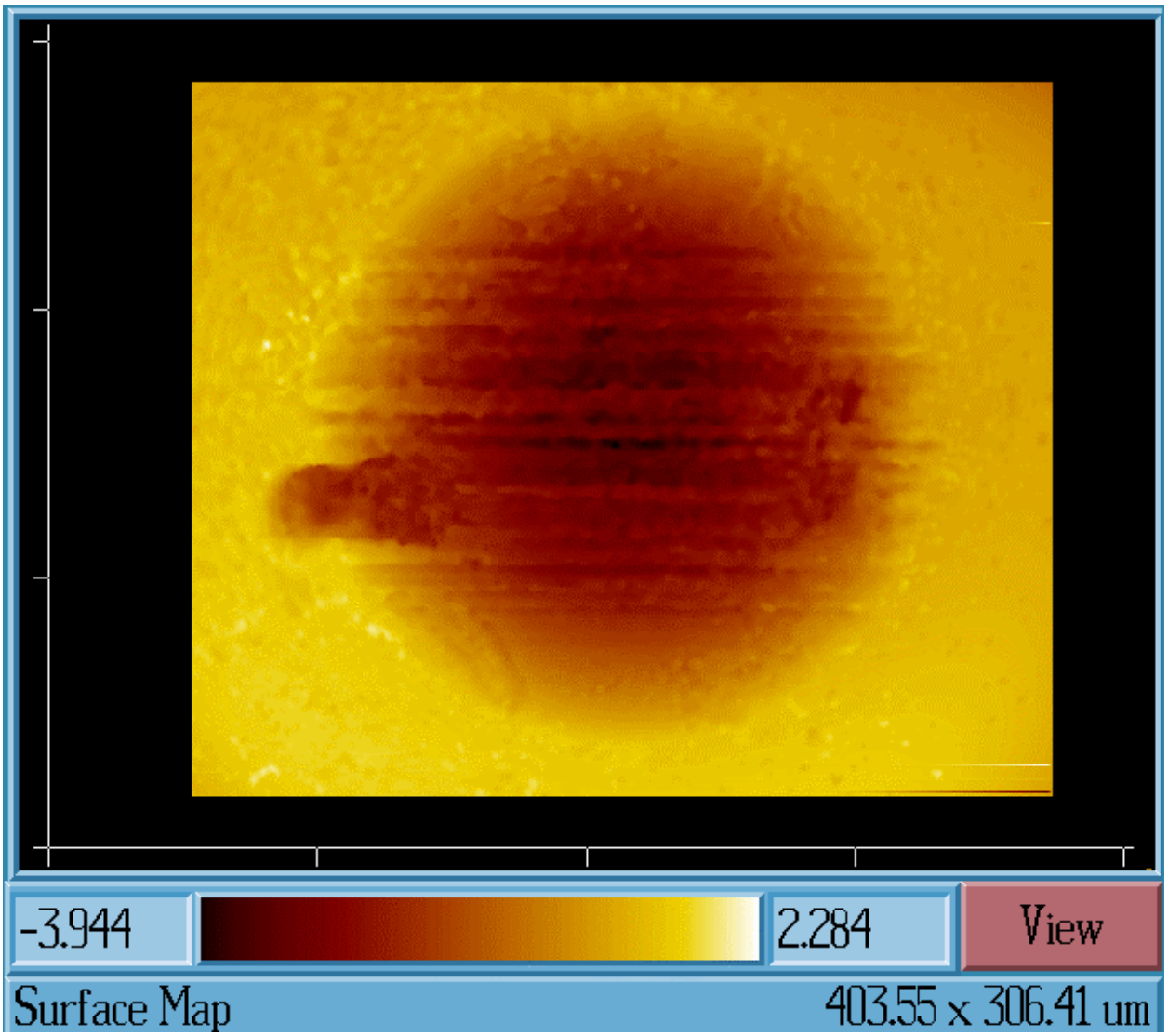

Figure 25. A 3-D surface profile showing a wear scar on an NFC2-coated fuel injector after a 1-million cycle lifetime test in Gasoline A.

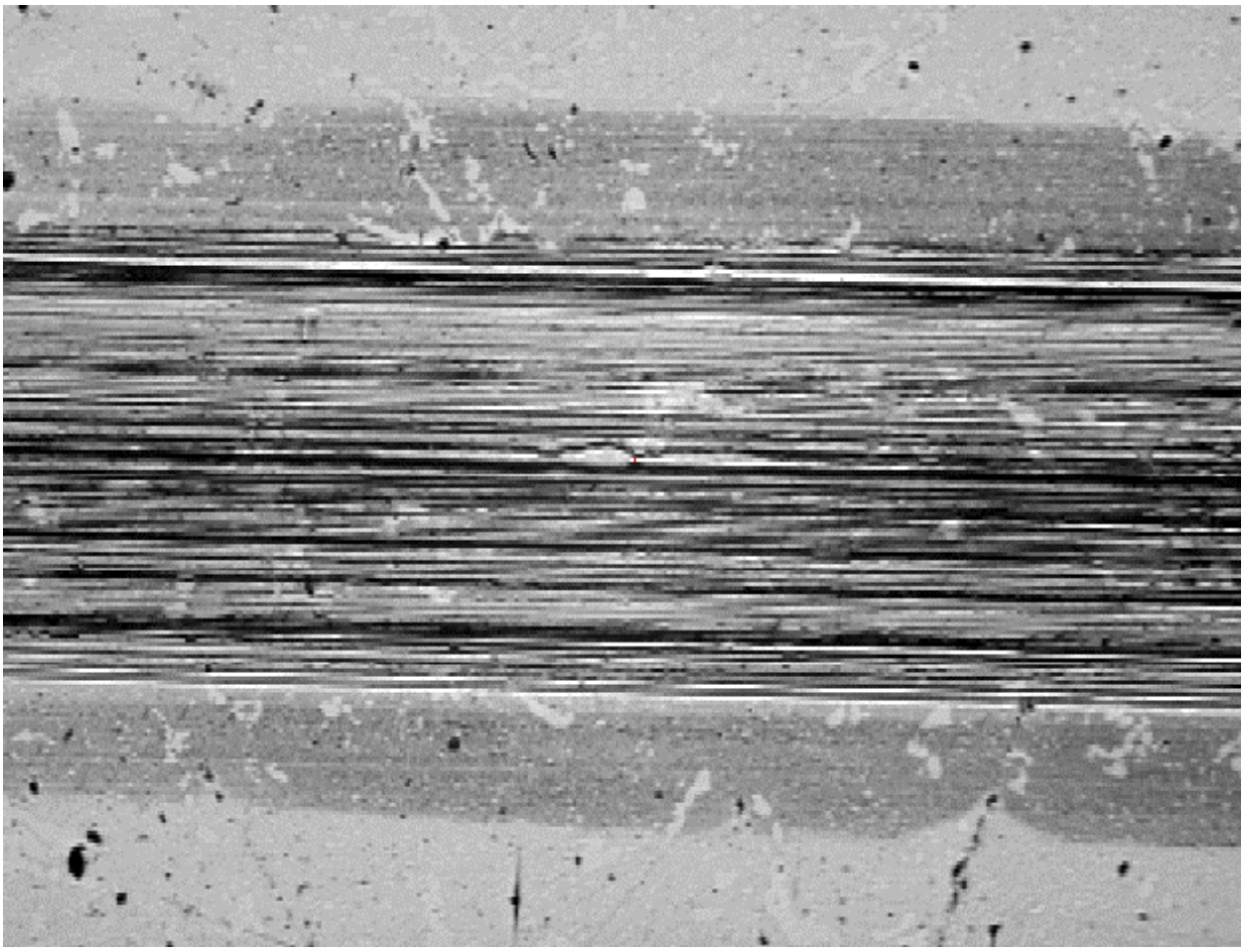

Figure 26. Optical micrograph of the steel flat worn against the NFC2-coated injector from Figure 25.

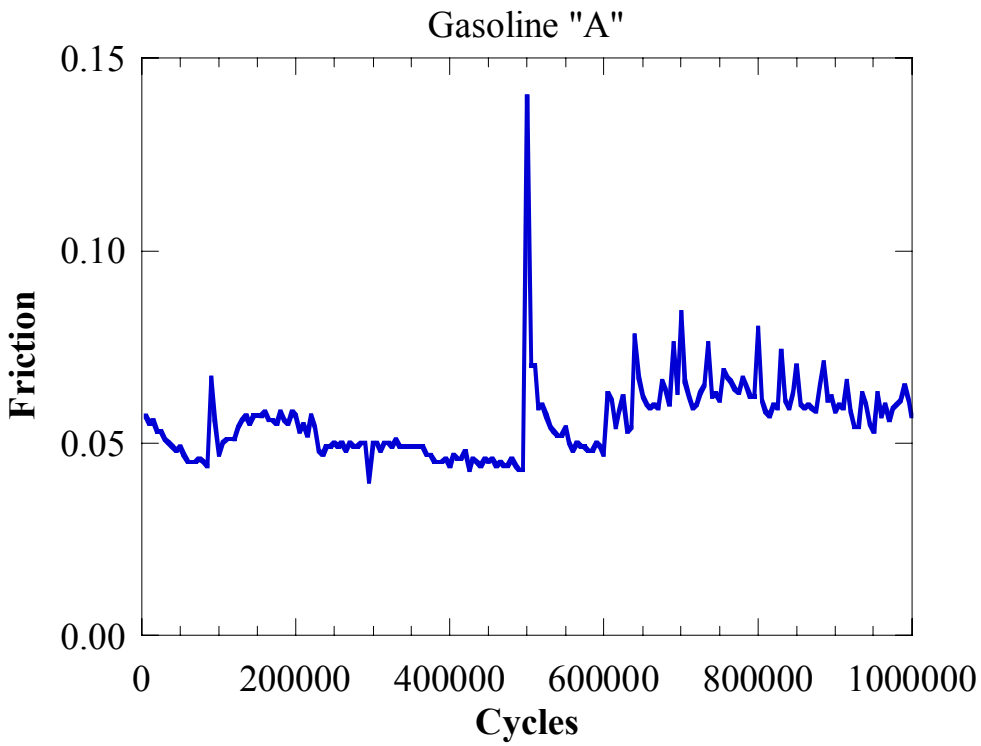

Figure 27. Friction trace of the 1-million cycle lifetime test of Figures 25 and 26.

Table 2. Fuels used in long-term reciprocating tests.

Name	Season	Type	Grade	Additive?
Ethanol	-	-	-	-
Gasoline A	Winter	Conventional	Premium	Yes
Gasoline B	Winter	Conventional	Premium	No
Gasoline C	Winter	Reformulated	Premium	Yes
Gasoline D	Summer	Reformulated	Premium	No
Gasoline E	Winter	Conventional	Regular	Yes
Gasoline F	Winter	Conventional	Regular	No
Gasoline G	Summer	Conventional	Regular	No

Table 3. Friction results for three surface treatments averaged over seven gasolines.

Surface treatment	Friction average	Improvement
Uncoated	0.29	
NFC-6	0.22	27% reduction over uncoated
NFC-2	0.15	48% reduction over uncoated

Table 4. Wear rates for three surface treatments averaged over seven gasolines, stated in terms of change from the uncoated case.

Surface treatment	Flat wear	Injector wear	Total wear
Uncoated	Baseline	Baseline	Baseline
NFC-6	-56% from uncoated	+13% from uncoated	-39% from uncoated
NFC-2	-77% from uncoated	+89% from uncoated	-36% from uncoated

E. BOTD Tests on Formulated Gasolines

A set of BOTD tests was performed with uncoated steel discs, per the standard test specification, to provide a measure of the lubricity of each of the gasolines used in the long-term reciprocating tests in Section V.D. Figure 28 on page 63 shows friction for Gasolines A through G, plus ethanol and the regular gasoline used in the short reciprocating tests of Section V.C. Figure 29 on page 64 gives the wear scar diameter from the tests.

The friction and wear results were quite consistent, with the low friction fuels also providing low wear. However, the differences in friction and wear among the fuels were relatively small. This was consistent with the observation in Section V.D that the gasoline type was not the major factor influencing wear. At first glance, the friction and wear results appeared inconsistent with the observation regarding the effects of the gasolines on friction and wear rate for injector-on-flat contacts. However, closer examination revealed that the differences were a result of inclusion of the coated materials in the results of Section V.D. Taking into account only the data from the uncoated injectors, to match the uncoated BOTD discs, resulted in complete consistency between the two sets of results.

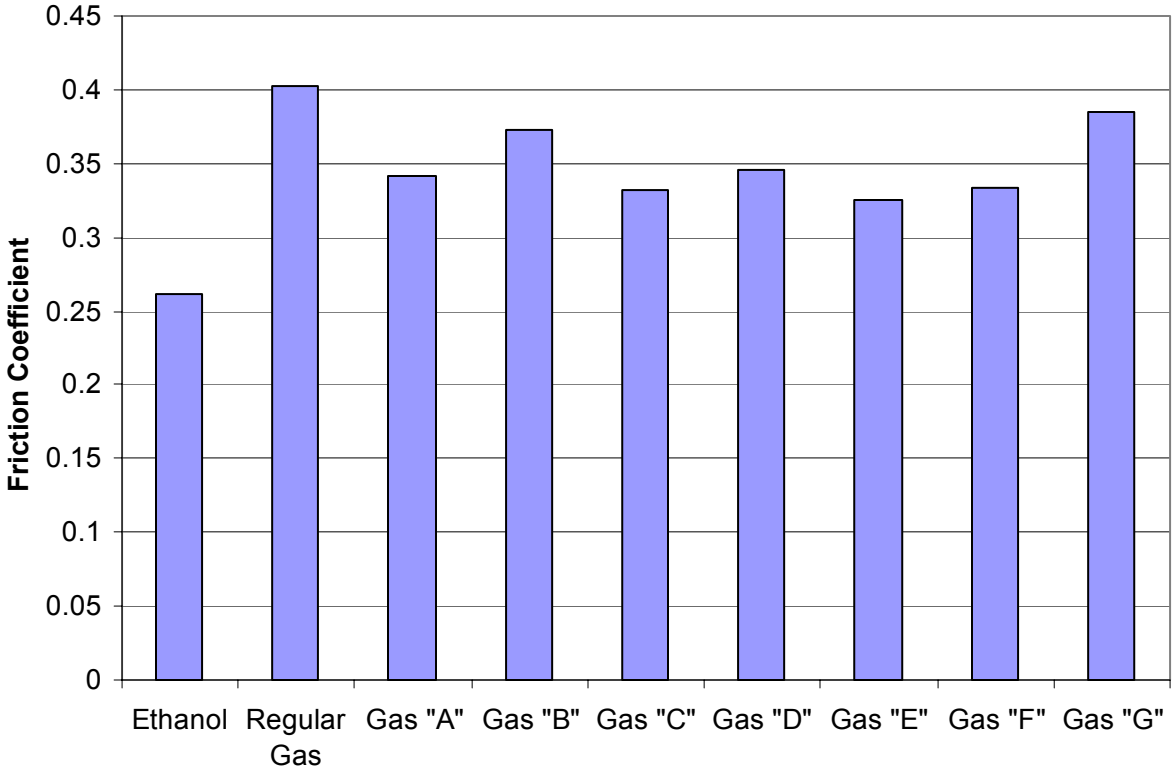

Figure 28. Friction from BOTD lubricity tests of uncoated steels against alumina balls in several gasolines.

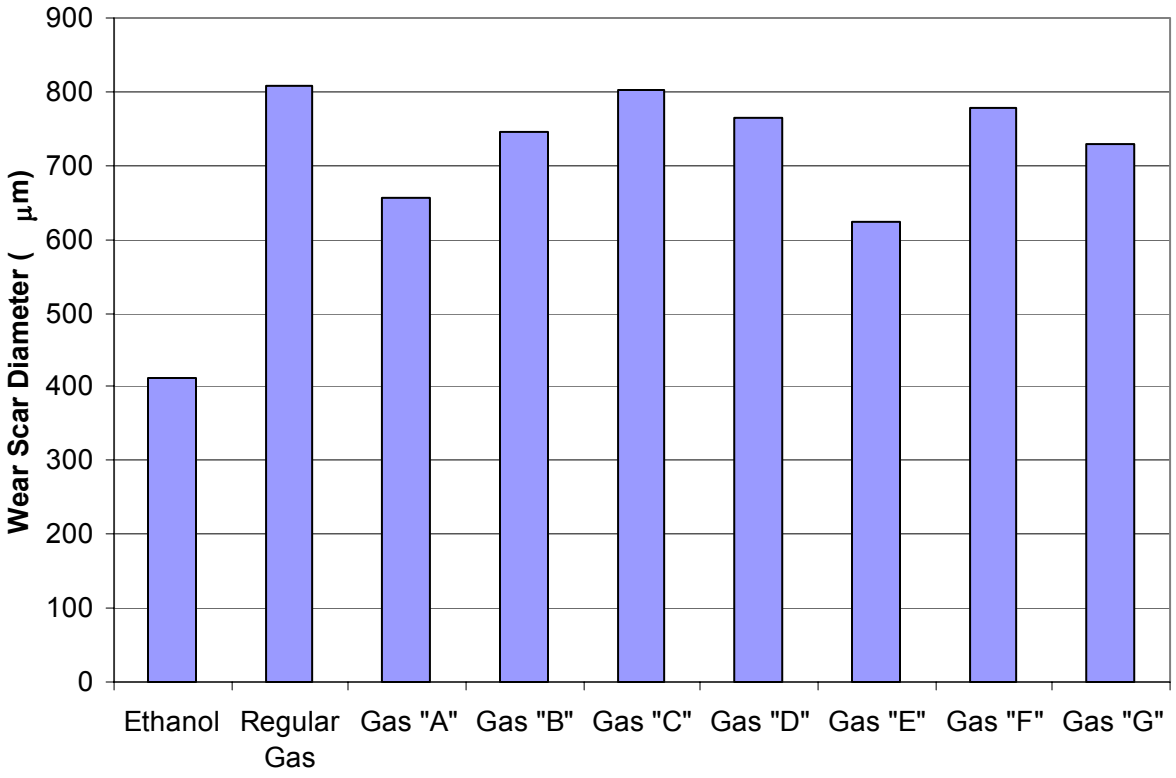

Figure 29. Wear scar diameter from BOTD lubricity tests in several gasolines.

F. Raman Characterization

Several Raman spectroscopy studies were performed to assist interpretation of the results of the wear tests. The responses from unworn areas of the coated injector and the steel flat were tested, as well as worn areas of each and, in some cases, wear debris. The gasoline from the wear test was not rinsed away with solvent to allow detection of any films which may have formed on the wear surfaces.

Figure 30 on page 67 shows the Raman intensity from several areas in a long reciprocating test of an NFC2-coated injector worn in Gasoline A. The response from a worn area of NFC2 coating (in blue) showed the two broad peaks typical of diamondlike carbon coatings. The red trace is from an area of the injector where the NFC was worn off and the steel substrate was exposed. The flat response is characteristic of steel, and there was no indication of any transfer film. This indicates that neither the gasoline nor the NFC was forming any protective chemical layer on the exposed steel. This wear reduction strategy is common in oils for boundary lubrication applications; many soft wear-resistant coatings such as MoS_2, operate by smearing across worn areas to protect the surface. The black trace in the plot is from a piece of wear debris found on the steel flat. The two low, broad peaks in this scan identified the debris as a piece of NFC.

Figure 31 on page 68 shows the Raman intensity from both worn and unworn areas of an NFC2-coated injector worn in Gasoline A. The two traces were substantially the same, indicating that the atomic structure of the NFC was not changed by the wear process. Similarly, Figure 32 on page 69 shows the Raman intensity from worn and unworn NFC2 tested in Gasoline B. Those scans were also essentially the same. This result eliminated the possibility that the NFC was wearing sacrificially by transforming into graphite, an example of a soft wear-

resistant solid of the type mentioned above. Graphite would appear in these Raman scans as much sharper peaks. Instead, NFC2 appeared to continue to protect against wear of the exposed steel simply by continuing to support the load around exposed substrate material.

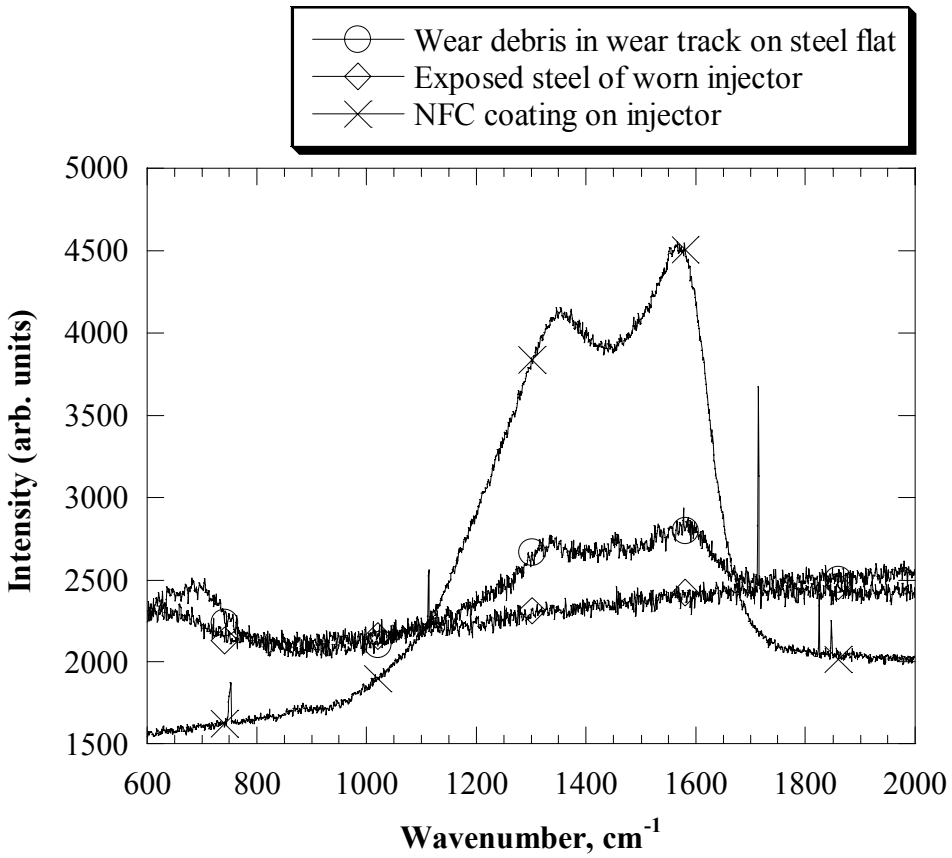

Figure 30. Raman spectroscopy scans of several areas after a 1-million cycle wear test of NFC2 in Gasoline A.

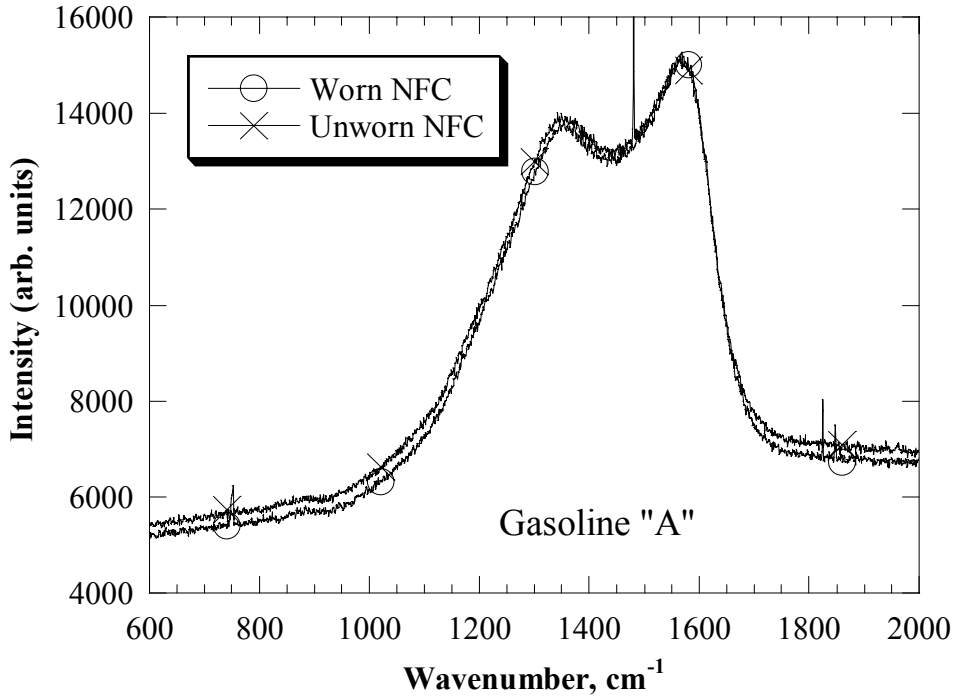

Figure 31. Raman spectroscopy scans of worn and unworn areas of an NFC2-coated injector tested in gasoline A.

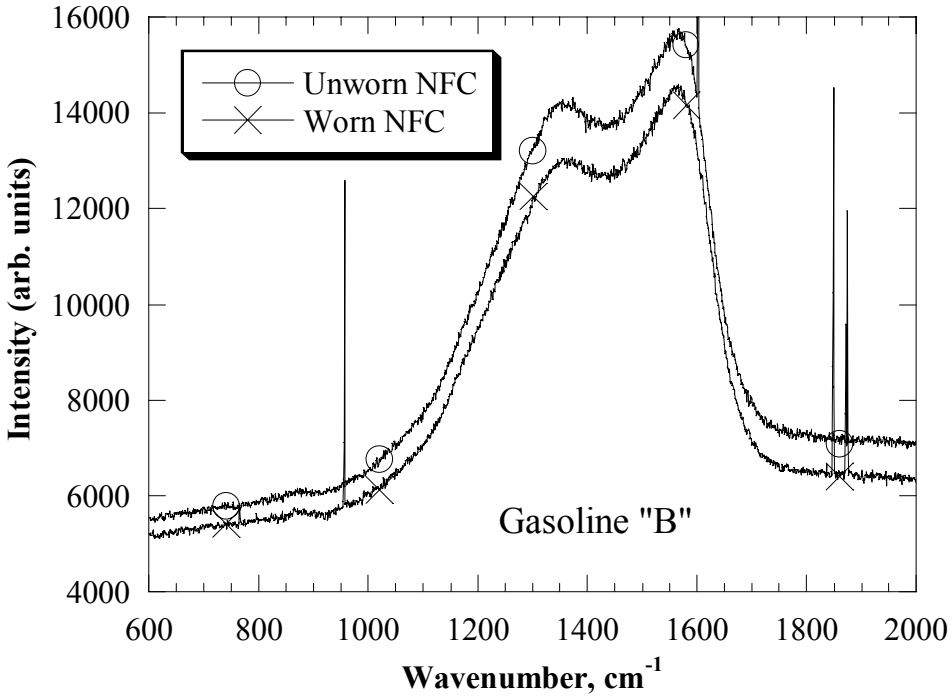

Figure 32. Raman spectroscopy scans of worn and unworn areas of an NFC2-coated injector tested in gasoline B.

G. Characterization of Residual Stress in NFC Coatings

As noted in the Approach (Section III.D.), residual in-plane stresses are an important property of coatings. Moderate tensile stresses or excessive compressive stresses can cause wear failure modes that do not occur in stress-free materials. Therefore, the residual stresses in the NFC coatings were characterized to verify their appropriateness for engine applications.

Figure 33 on page 73 plots the residual in-plane stresses in three varieties of NFC as measured by laser scanning. Two thicknesses of each type of coating were studied. In addition to NFC2 and NFC6, a third coating type (NFC7) was included in this study. NFC7 was simply a coating made by another variation on the deposition process parameters that led to NFC2 and NFC6. In Figure 33, the thickness of each coating is given with each bar representing the stress level. The stress bars of the plot are mostly negative, implying compressive stresses (positive stresses are tensile).

Qualitatively, the NFC6 coatings displayed the lowest values of residual stress, followed by NFC2 and NFC7. Stress was lower in the thicker NFC2 and NFC7 coatings, implying some change in coating properties with thickness. In terms of functionality, the stresses in NFC6 and NFC2 would not have been expected to degrade their wear performance. The tensile stress in the thin NFC6 coating was too small to significantly encourage crack opening, and the compressive stresses in the NFC2 coatings were not large enough to create any danger of failure by spallation. This is consistent with the wear mechanisms observed in the tribological testing in this work. The compressive stresses displayed by the NFC7 coatings, however, were comparatively large and may have resulted in spalling in some circumstances, depending on the toughness of the coating.

The residual stress results also provided information on the structure of the NFC coatings. The mechanisms by which metal and ceramic coatings acquire and retain stress are well understood and can be applied to the case of diamondlike carbon coatings such as NFCs. These covalently bonded materials generally contain residual stresses created by three mechanisms.[47] The first is due to the mismatch in coefficient of thermal expansion between the coating and substrate, and the difference in temperatures between deposition, ambient, and service conditions. The second mechanism is tensile stresses that appear across voids in the material, commonly seen in rapidly deposited metal films. The third is compressive stresses created by energetic bombardment by ions during deposition, for example, stresses caused by a bias like that used in deposition of NFC. The ion bombardment not only adds atoms to the already-solidified structure, increasing its volume, but also displaces atoms in the structure from their low-energy positions into other places. The latter also increases the volume of the structure. In metals, increasing flux or energy of bombardment adds compressive stress up to the yield strength of the metal. In ceramics, yield strengths are very, high and compressive residual stresses of 3-10 GPa are not uncommon. Such coatings often fail by spalling or delamination.

In the case of the NFC coatings, the magnitudes of the residual stresses were in the low end of the range for diamondlike carbon coatings. This is because many DLCs are deposited in such a way that a highly crosslinked, hydrogen-poor or -free structure rich in sp^3 carbon-carbon bonds is created. Such structures are hard and, therefore, support large residual stresses. The deposition process used to create NFCs incorporated a significant amount of hydrogen into the coating structure, reducing its hardness (although it is still harder than tool steel[48]) and its capacity to retain large residual stresses. On the basis of the stress variations from coating to coating in the NFC family, the strength of the crosslinked sp^3 network increased from NFC6 to

NFC2 and finally was greatest in NFC7. The benefit of this has been that NFC2 and NFC6 were well adapted to mechanical applications.

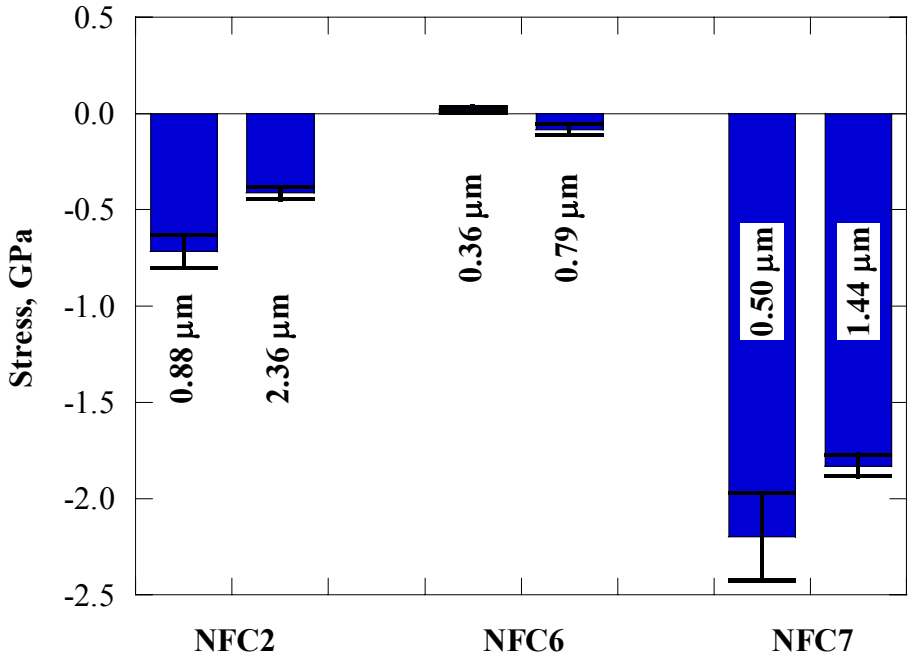

Figure 33. Residual in-plane stresses in three varieties of NFC coating having two thicknesses.

VI. DISCUSSION

The standardized BOTD lubricity tests and customized reciprocating wear tests were in general agreement as to the benefit of using NFC coatings in an engine environment. The lubricities of the formulated gasolines tested with uncoated BOTD discs were also consistent with the wear rates observed in reciprocating wear tests using uncoated materials. Differences in the results between the two types of tests were attributable to a number of factors. First, the peak and average Hertzian contact pressures in the BOTD tests were approximately half those in the reciprocating tests. The average velocities were similar, but the local thermal situation in the two tests were very different. In the BOTD test the counterface was made of Al_2O_3 and was rotating; the Al_2O_3 was cooled because of its moderate thermal conductivity and exposure to liquid. In the reciprocating tests, only one area of the counterface was worn, and that area was in constant contact with the flat. Flats in the BOTD tests, on the other hand, were in constant contact with the counterface, while in the reciprocating tests they were not. Comparisons might be made between the BOTD wear rates and the wear rates of the injectors in reciprocating tests, except for the fact that the BOTD tests were performed in laboratory air and the reciprocating tests were performed under nitrogen to better simulate the operating conditions of fuel injectors. The presence of water vapor and oxygen could have significantly affected wear. Another significant difference between the two techniques was the tendency for debris to remain in the wear track. In reciprocating tests, debris tended to be pushed out the ends of the track, while in BOTD tests it remained in the wear track unless it fell out sideways, in which case it joined the circulating fluid. Nonetheless, NFC coatings provided considerable protection against wear in the initial BOTD tests as well as in the reciprocating tests. For regular gasoline, NFC reduced the BOTD wear rate by approximately a factor of 70.

Based on the optical microscopy from the samples in the BOTD wear tests, it was determined that the adhesion between the steel discs and the NFC coating was failing when the NFC was worn very thin. Steps were taken to modify the deposition technique for coating NFC onto future steel flats and injectors, and this problem did not recur.

In the initial reciprocating tests of NFC-coated flats worn in ethanol and gasoline (Section V.B.), no wear at all was observed. On the other hand, in the subsequent work, such as the systematic study at standard fuels in Section V.C., wear rates in the low 10^{-8} $mm^3/N \cdot m$ range were measured for the flat and sometimes the injector. This discrepancy could have been due to two factors. First, the track length (and, therefore, the total sliding distance and average velocity) was increased from 200 μm to 1 mm in the later study, thereby increasing both the contact severity and the sliding distance over which contact was maintained. Second, the lowest wear rate reported in the earlier study was in the mid 10^{-7} $mm^3/N \cdot m$ range (see Figure 7). More effective use of the 3-D optical surface profiler may have allowed the detection of these extremely small wear scars in the later study.

Another difference correlating with the increase in severity between the two sets of experiments was bumps of added material on the counterfaces in the earlier (less severe) tests of bare steel parts in ethanol and gasoline. These bumps were not observed in the later tests, which implies that the protective oxidation/polymerization and/or debris reattachment could not be maintained under the more severe conditions of the second set of tests.

The comparison between NFC coatings and three commercial DLCs showed that the former were generally the best choice for reducing friction and wear, although Commercial DLC1 rivaled the NFC performances in several tests. Commercial DLC2 and 3 displayed poor performance under certain conditions, such as unlubricated or ethanol-lubricated wear. Between

NFC2, NFC6, and Commercial DLC1, each achieved the lowest wear rates in different test conditions. NFC6 performed the best in dry or ethanol-lubricated wear, Commercial DLC1 performed the best when lubricated by E85 or M85 fuel, and NFC2 had the best performance in regular gasoline. Arguably these differences could allow the coatings to be tailored for use in different environments. However, the most relevant condition for fuel injector applications was obviously the tests in regular gasoline, for which NFC2 provided both the best friction and the lowest wear rate.

When examining liquid-to-liquid variations for each coating, we noted that NFC2 reduced friction in all liquids compared to tests of uncoated materials in the same fluids, and that NFC6 did also but not to as great an extent. The wear rates for tests where a liquid lubricant was present were improved by a factor of three to four when NFC2 coatings were applied compared to uncoated surfaces. M85 fuel was the most aggressive in terms of causing wear, which may be attributable to the large amount of oxygen present in the methanol. The decrease of friction for coated surfaces compared to uncoated surfaces indicated that solid-solid contact was indeed taking place, in other words, the contact severity was not in the elastohydrodynamic regime where the load is entirely supported by the fluid.

The long-duration tests designed to determine the ultimate wear lifetime of the NFC coatings on injectors in current- and next-generation gasolines were analyzed for trends. By averaging the friction results for each coating over the seven gasolines used, found that NFC6 provided 27% lower friction on average, while NFC2 reduced friction by nearly a factor of two.

Applying NFC coatings on the injectors also provided clear improvements in total wear rate and wear rate of the flats compared to the uncoated injectors. In the case of the coated injectors themselves, NFC6 provided a wear rate very similar to that of the uncoated surface,

while the NFC2 coating wore significantly faster than NFC6 and the uncoated part. Taking into account the extremely low friction provided by NFC2 in the tests, we speculate that the NFC2 may have been slowly sacrificing itself to reduce both friction and counterface wear. In contrast, NFC6 provided reductions of both friction and wear nonsacrificially. This finding stands in contrast to the results from tests of wear rates in regular gasoline, where not only NFC6 but also the NFC2 provided flat and injector wear rates much improved over uncoated samples. Note that these wear rates were expressed as averages over the seven gasolines, and there were cases where the wear rate of NFC2-coated injectors was less than that of the uncoated injectors. The tests with regular gasoline may have been one such case. Nonetheless, both NFC coatings considerably reduced the total wear rate and the wear rate of the flats compared to uncoated surfaces. In fact, NFC2 provided better flat protection than NFC6, almost a factor of four improvement over uncoated samples. This coating may ultimately be beneficial in applications where the geometry of the mating (uncoated) part is of paramount importance, for example, the nozzle of a fuel injector carefully shaped to control the fuel spray characteristics.

Analysis of the friction and wear data by averaging the results for each gasoline over the three coatings used did not illuminate any clear trends. The average results for each gasoline were similar, but each was associated with a large error bar. The major factor influencing both the friction and the wear was the coating, not the gasoline.

The wear mechanisms operating in these tests were consistent with the observations from the analysis of residual stresses in the NFC coatings. The low-magnitude compressive residual stresses retarded crack opening but were too small to cause spallation or delamination. The adhesion issues in the pilot study using the BOTD tester were not a problem in the reciprocating tests. The wear mode in the gasolines seems to have been gradual removal of both the NFC and

the flat material by a slow polishing mechanism until the steel substrate was exposed. Exposed steel wore by oxidation and ejection of debris, which damaged nearby steel and coating material, but the NFC still supported part of the load and reduced the wear rate even after its thickness was worn through. Raman characterization of worn and unworn surfaces did not produce any evidence of a transfer film originating from the NFC, either on the steel flat or on the exposed steel substrate. The Raman data also did not show any graphitization of the NFC during wear, supporting the hypothesis that the wear mode is mechanical polishing rather than phase transformation.

The relevance of this work to the current research needs of the OAAT SIDI program, as defined by the OTT report Research Needs Related to Fuel Injection Systems in CIDI and SIDI Engines, can be seen by comparing these results to the research needs from that report, which are listed in Section I.C. Rate shaping, multiple injections, and other diesel-like strategies in injector design may create fatigue and wear issues due to the increase in speed and number of injector tip/orifice contacts per engine cycle, and coatings such as NFC can be used to address those issues. In terms of deposit formation, modification of the surface chemistry of the injector through the use of a nonferrous coating may forestall or prevent the initial stages of deposit formation. This work may be regarded as enabling that step by showing that NFC coatings are compatible with the other demands on fuel injectors.

This work directly addressed issues in injector materials and parasitic losses by investigating the effect of fuel additives on friction and wear and attempting to reduce friction in gasoline-lubricated parts, which certainly include those not exposed to combustion such as pumps. Quality control and scale-up challenges have been a constant influence on Argonne's work on NFC. The ANL Tribology Group has obtained a commercial-scale coating system and

is working to adapt NFC technology to it in order the coating system's manufacturer will be able to offer NFC systems to parts manufacturers.

VII. CONCLUSIONS

The following conclusions were reached:

- Argonne's NFC coatings consistently reduced friction and wear in existing and reformulated gasolines.
- Compared to three commercial DLC coatings, NFC provided the best friction reduction and protection from wear in gasoline and alternative fuels.
- NFC was successfully deposited on production fuel injectors.
- Customized wear tests were performed to simulate the operating environment of fuel injectors.
- Industry standard lubricity test results were consistent with customized wear tests in showing the friction and wear reduction of NFC and the lubricity of fuels.
- Failure of NFC coatings by tensile crack opening or spallation did not occur, and issues with adhesion to steel substrates were eliminated.
- This work addressed several of the current research needs of the OAAT SIDI program, as defined by the OTT report Research Needs Related to Fuel Injection Systems in CIDI and SIDI Engines.

VIII. ACKNOWLEDGMENTS

The authors are grateful for the support for this project which came from Rogelio Sullivan of the Office of Advanced Automotive Technologies (OAAT) within the U.S. Department of Energy's Office of Transportation Technologies (OTT).

The authors wish to thank the following undergraduate student interns at ANL for performing many of the wear tests: Kristen Holverson, Joanne Lee, Weronika Walkosz, and Matt Siniawski. We also wish to thank Russell Bosch and Michael Seino of Delphi Automotive Systems, and John Weber and Robert Gerry of BP Amoco for helpful discussions, Robert A. Erck of ANL for his part in design and construction of the Fretting Tester, and Anirudha V. Sumant for his assistance with the Raman spectroscopy.

REFERENCES

[1] Research Needs Related To Fuel Injection Systems In CIDI And SIDI Engines, ed. R. R. Fessler, G. R. Fenske, R. M. Cuenca, R. M. Nault, Argonne National Laboratory, 2001.

[2] C. S. Lee, K. H. Lee, M. S. Chon, and D. S, Kim, Atomization and Sprays **11,** 2001, 35.

[3] S. Henriot, A. Chaouche, E. Cheve, and J.-M. Duclos, Oil & Gas Science and Technology - Rev. IFP **54** (2), 1999, 279.

[4] J. Li, Y. Huang, T. F. Alger, R. D. Matthews, M. J. Hall, R. H. Stanglmaier, C. E. Roberts, W. Dai, and R. W. Anderson, Journal of Engineering for Gas Turbines and Power **123**, 2001, 659.

[5] C. Habchi, H. Foucart, and T. Baritaud, Oil & Gas Science and Technology - Rev. IFP **54** (2), 1999, 211.

[6] F. Zhao, M.-C. Lai, and D. L. Harrington, Progress in Energy and Combustion Science **25**, 1999, 437.

[7] S. C. Hill and L. Douglas Smoot, Progress in Energy and Combustion Science **26**, 2000, 417.

[8] H. Richter and J. B. Howard, Progress in Energy and Combustion Science **26**, 2000, 565.

[9] D. E. Hall and C. J. Dickens, SAE 1999-01-3530.

[10] J. Cousin, W. M. Ren, and S. Nally, Oil & Gas Science and Technology - Rev. IFP **54** (2), 1999, 227.

[11] W. Hentschel, Proceedings of the Combustion Institute **28**, 2000, 1119.

[12] R. B. Wicker, H. I. Loya, P. A. Hutchison, and J. Sakakibara, SAE 1999-01-3535.

[13] D. P. Wei, H. A. Spikes, and S. Korcek, Tribology Transactions **42** (4), 1999, 813.

[14] W. D. Ping, S. Korcek, and H. Spikes, SAE 962010.

[15] M. Nikanjam, SAE 1999-01-1479.

[16] ISO 12156-1 and ISO 12156-2, Diesel fuel--assessment of lubricity using the high-frequency reciprocating rig (HFRR).

[17] P. I. Lacey, Tribology Transactions **37** (2), 1994, 253.

[18] E. A. Bardasz, D. C. Arters, E. A. Schiferl, and D. W. Righi, SAE 1999-01-1499.

[19] S. C. Tung and S. I. Tseregounis, SAE 2000-01-1781.

[20] Y. Wakuri, M. Soejima, Y. Ejima, T. Hamatake, and T. Kitahara, SAE 952471.

[21] Y. S. Wang, S. K. Schaefer, C. Bennett, and G. C. Barber, SAE 952476.

[22] A. Ito, L. Yang, and H. Negishi, SAE 982663.

[23] A. Gorel, K. Voss, and G. Austell, SAE 1999-01-3666.

[24] A. Hultqvist, M. Christensen, and B. Johansson, SAE 2000-01-1833.

[25] R. Gahlin, M. Larsson, and P. Hedenqvist, Wear **249**, 2001, 302.

[26] A. Erdemir, O. Ozturk, M. Alzoubi, J. Woodford, L. Ajayi, and G. Fenske, SAE 2000-01-0518.

[27] A. Erdemir, F. A. Nichols, X. Z. Pan, R. Wei, and P. Wilbur, Diamond and Related Materials **3** (1-2), 1994, 119.

[28] E. I. Meletis, A. Erdemir, and G. R. Fenske, Surface and Coatings Technology **73** (1-2), 1995, 39.

[29] Y. Liu, A. Erdemir, and E. I. Meletis, Surface and Coatings Technology **86-7** (1-3), 1996, 564.

[30] A. Erdemir, G. R. Fenske, J. Terry, and P. Wilbur, Surface and Coatings Technology **94-5** (1-3), 1997, 525.

[31] A. Erdemir, O. L. Erlimaz, and G. Fenske, Journal of Vacuum Science and Technology A - Vacuum Surfaces and Films **18** (4), 2000, 1987.

[32] A. Erdemir, O. L. Eryilmaz, I. B. Nilufer, and G. R. Fenske, Diamond and Related Materials **9** (3-6), 2000, 632.

[33] A. Erdemir, I. B. Nilufer, O. L. Eryilmaz, M. Beschliesser, and G. R. Fenske, Surface and Coatings Technology **121**, 1999, 589.

[34] D. A. Ersoy, M. J. McNallan, Y. Gogotsi, and A. Erdemir, Tribology Transactions **43** (4), 2000, 809.

[35] A. Erdemir, C. Bindal, J. Pagan, and P. Wilbur, Surface and Coatings Technology **77** (1-3), 1995, 559.

[36] Y. Liu, A. Erdemir, and E. I. Meletis, Surface and Coatings Technology **82** (1-2), 1996, 48.

[37] A. Erdemir, C. Bindal, G. R. Fenske, C. Zuiker, and P. Wilbur, Surface and Coatings Technology **86-7** (1-3), 1996, 692.

[38] A. Erdemir, C. Bindal, G. R. Fenske, and P. Wilbur, Tribology Transactions **39** (3), 1996, 735.

[39] Y. Liu, A. Erdemir, and E. I. Meletis, Surface and Coatings Technology **94-5** (1-3), 1997, 463.

[40] A. Erdemir, O. L. Eryilmaz, I. B. Nilufer, and G. R. Fenske, Surface and Coatings Technology **133**, 2000, 448.

[41] J. A. Heimberg, K. J. Wahl, I. L. Singer, and A. Erdemir, Applied Physics Letters **78** (17), 2001, 2449.

[42] A. Erdemir and G. R. Fenske, Tribology Transactions **39** (4), 1996, 787.

[43] O. O. Ajayi, M. F. Alzoubi, A. Erdemir, and G. R. Fenske, Tribology Transactions **44** (2), 2001, 298.

[44] M. F. Alzoubi, O. O. Ajayi, J. B. Woodford, A. Erdemir, and G. R. Fenske, Tribology Transactions **44** (4), 2001, 591.

[45] P. A. Flinn, D. S. Gardner, and W. D. Nix, IEEE Trans. on Electron Devices **ED-34** (3), 1987, 689.

[46] G. G. Stoney, Proceedings of the Royal Society of London A: Materials **82**, 1909, 172.

[47] H. Windischmann, Critical Reviews in Solid State and Materials Sciences **17** (6), 1992, 547.

[48] D. Ersoy, unpublished data.